

1-1-2008

A Cfd model to predict pressure loss coefficient in circular ducts with a motorized damper

Pallavi Annabattula
University of Nevada, Las Vegas

Follow this and additional works at: <https://digitalscholarship.unlv.edu/rtds>

Repository Citation

Annabattula, Pallavi, "A Cfd model to predict pressure loss coefficient in circular ducts with a motorized damper" (2008). *UNLV Retrospective Theses & Dissertations*. 2390.
<http://dx.doi.org/10.25669/paqq-wgwd>

This Thesis is protected by copyright and/or related rights. It has been brought to you by Digital Scholarship@UNLV with permission from the rights-holder(s). You are free to use this Thesis in any way that is permitted by the copyright and related rights legislation that applies to your use. For other uses you need to obtain permission from the rights-holder(s) directly, unless additional rights are indicated by a Creative Commons license in the record and/or on the work itself.

This Thesis has been accepted for inclusion in UNLV Retrospective Theses & Dissertations by an authorized administrator of Digital Scholarship@UNLV. For more information, please contact digitalscholarship@unlv.edu.

A CFD MODEL TO PREDICT PRESSURE LOSS COEFFICIENT IN CIRCULAR
DUCTS WITH A MOTORIZED DAMPER

by

Pallavi Annabattula E.I

Bachelor of Engineering
Andhra University College of Engineering, Visakhapatnam, India
2006

A thesis submitted in partial fulfillment
of the requirements for the

**Master of Science Degree in Mechanical Engineering
Department of Mechanical Engineering
Howard R. Hughes College of Engineering**

**Graduate College
University of Nevada, Las Vegas
December 2008**

UMI Number: 1463493

INFORMATION TO USERS

The quality of this reproduction is dependent upon the quality of the copy submitted. Broken or indistinct print, colored or poor quality illustrations and photographs, print bleed-through, substandard margins, and improper alignment can adversely affect reproduction.

In the unlikely event that the author did not send a complete manuscript and there are missing pages, these will be noted. Also, if unauthorized copyright material had to be removed, a note will indicate the deletion.

UMI[®]

UMI Microform 1463493

Copyright 2009 by ProQuest LLC.

All rights reserved. This microform edition is protected against unauthorized copying under Title 17, United States Code.

ProQuest LLC
789 E. Eisenhower Parkway
PO Box 1346
Ann Arbor, MI 48106-1346



Thesis Approval

The Graduate College
University of Nevada, Las Vegas

September 23, 2008

The Thesis prepared by

Pallavi Annabattula


Entitled

A CFD Model to Predict Pressure Loss Coefficient in Circular
Ducts with a Motorized Damper

is approved in partial fulfillment of the requirements for the degree of

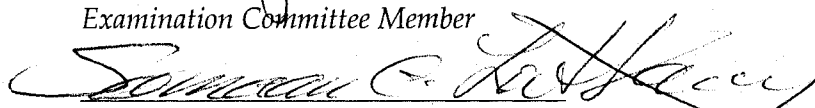
Master of Science in Mechanical Engineering


Examination Committee Chair


Dean of the Graduate College


Examination Committee Member


Examination Committee Member


Graduate College Faculty Representative

ABSTRACT

A CFD Model to Predict Pressure Loss Coefficient in Circular Ducts with a Motorized Damper

by

Pallavi Annabattula

Samir F Moujaes, Ph.D., P.E., Examination Committee Chair
Professor, Department of Mechanical Engineering
University of Nevada, Las Vegas

The pressure loss coefficient was determined for a circular duct with a circular damper using computational fluid dynamics. The CFD package Star-CD was used to predict the air flow and pressure distribution in the duct. A three dimensional computational fluid dynamics model was developed and simulated for five different positions of the damper ranging from partially opened position to completely opened position. The available standard k- ϵ model for high Reynolds number was used. The duct was also simulated for different flow conditions by varying the Reynolds number. The code generated the pressure drop across the damper, which was used to compute the pressure loss coefficient.

The model was initially tested for grid independency. A diameter along the cross-section downstream of the damper was considered and the velocity component in the direction of the flow was verified for the grid independency. The mesh size of 400,000 cells obtained from grid independency was used for all the models. The pressure loss coefficient determined varied considerably with the damper angle. The pressure loss

coefficient was high at low angles of opening indicating greater pressure losses. The Reynolds number had little impact on the k-factors. The predicted values were also compared with previous studies and were found to be in general good agreement. The knowledge of the pressure losses and the pressure loss coefficient can be used as a parameter for the direct digital control of the HVAC systems in order to obtain better efficient systems.

TABLE OF CONTENTS

ABSTRACT.....	iii
TABLE OF CONTENTS.....	v
LIST OF FIGURES	vi
ACKNOWLEDGEMENTS.....	vii
CHAPTER 1 LITERATURE REVIEW	1
CHAPTER 2 INTRODUCTION AND BACKGROUND	4
2.1 Background.....	4
2.1.1 Dampers	4
2.1.2 Damper Actuator.....	4
2.1.3 Types of Dampers	5
2.1.4 Damper Sizing	9
2.1.5 Damper Losses.....	10
2.1.6 Applications of Dampers	11
2.2 Significance of the Research.....	12
CHAPTER 3 NUMERICAL MODELING OF DAMPER	15
3.1 Computational Fluid Dynamics.....	15
3.2 Star-CD	17
3.2.1 Pro-surf	17
3.2.2 Pro-am.....	18
3.2.3 Pro-star	18
3.3 Model Description	19
CHAPTER 4 RESULTS AND DISCUSSIONS	23
4.1 CFD Simulations.....	23
4.1.1 Grid Independency Results.....	23
4.1.2 CFD Simulations Results.....	26
4.1.3 Prediction of Pressure Loss Coefficients	41
CHAPTER 5 CONCLUSIONS	47
REFERENCES	49
VITA	52

LIST OF FIGURES

Figure 2 - 1 Butterfly Damper (source www.famcomfg.com/images/BD.gif).....	5
Figure 2 - 2 Gate Damper (source tapseis.anl.gov/.../Gate_Valve_Diagram.jpg).....	6
Figure 2 - 3 Split Damper	7
Figure 2 - 4 Parallel Blade Dampers.....	8
Figure 2 - 5 Opposed Blade Dampers.....	8
Figure 3 - 1 Schematic of the duct with a single-blade damper.....	19
Figure 3 - 2 Model with tetrahedral mesh for simulation	20
Figure 4 - 1 Cross-section of the duct considered for grid independency test.....	23
Figure 4 - 2 Z-component of velocity (m/s) along a diameter parallel to the direction of the damper axis	25
Figure 4 - 3 Z-component of velocity (m/s) along a diameter normal to the direction of the damper axis	26
Figure 4 - 4 Velocity (m/s) vector plot for 30 degree damper opening at $Re=30000$	27
Figure 4 - 5 Velocity (m/s) vector plot downstream of the damper at 30 degree $Re=30000$	28
Figure 4 - 6 Pressure (Pa) profile for 30 degree damper opening at $Re=30000$	29
Figure 4 - 7 Velocity vector plot for 30 degree damper opening at $Re=45000$	30
Figure 4 - 8 Pressure profile for 30 degree damper opening at $Re=45000$	31
Figure 4 - 9 Velocity vector plot for 30 degree damper opening at $Re=60000$	32
Figure 4 - 10 Pressure profile for 30 degree damper opening at $Re=60000$	32
Figure 4 - 11 Velocity vector plot for 30 degree damper opening at $Re=75000$	33
Figure 4 - 12 Pressure profile for 30 degree damper opening at $Re=75000$	34
Figure 4 - 13 Velocity vector plot for 30 degree damper opening at $Re=90000$	35
Figure 4 - 14 Pressure profile for 30 degree damper opening at $Re=90000$	35
Figure 4 - 15 Gauge static pressure along the duct for 30 deg damper angle.....	36
Figure 4 - 16 Velocity vector plot for 45 degree damper opening at $Re=30000$	37
Figure 4 - 17 Pressure profile for 45 degree damper opening at $Re=30000$	38
Figure 4 - 18 Pressure profile for 90 degree damper opening at $Re=30000$	39
Figure 4 - 19 Static gauge pressure along the duct at 15 & 30 degrees $Re=30000$	40
Figure 4 - 20 Static gauge pressure along the duct at 45 & 90 degrees $Re=30000$	40
Figure 4 - 21 Comparison of k-factors at 15 and 30 deg damper opening	42
Figure 4 - 22 Comparison of k-factors at 45, 60 and 90 degree damper opening	43
Figure 4 - 23 Comparison of k-factors at $Re=90000$	44
Figure 4 - 24 Comparison of k-factors at $Re=30000$	44
Figure 4 - 25 Comparison of k-factors at $Re=45000$	45
Figure 4 - 26 Comparison of k-factors at $Re=60000$	45
Figure 4 - 27 Comparison of k-factors at $Re=75000$	46

ACKNOWLEDGEMENTS

I would like to express my deepest appreciation to Dr. Samir Moujaes for his help and guidance in the completion of my thesis and through out my graduate program. It has been very rewarding and satisfying experience to be able to work with a person of such vast knowledge and experience. I would like to thank my committee member, Dr. Robert Boehm for his assistance and timely guidance throughout my Master's program. I would also like to thank my committee members, Dr. Woosoon Yim and Dr. Saman Ladkany for their support, patience, and effort in reviewing my thesis.

This thesis has been a challenging experience to me and was accomplished through the help of many people. Briefly mentioning their names does not completely express my gratitude towards them. In particular, I extend my appreciation and thanks to graduate students, Sucharita Akula and Kiran Mohan Veepuri for their help during the model development and analysis. I thank the Department of Mechanical Engineering, UNLV, for providing me financial support through out the coursework and for providing timely support and infrastructure to finish my thesis. I would like to thank the students and staff at Mechanical Engineering department for all the help and support in completing this thesis.

Last but not the least, I would like to thank my family and friends, and all the other people whom I have not mentioned above but have helped me in some way through the completion of my thesis degree.

CHAPTER 1

LITERATURE REVIEW

The proper estimation of pressure loss coefficients in ducts is of significant value as it highly affects the fan sizing and the overall energy efficiency of the air distribution system. The available data from sources like ASHRAE is limited and generic in nature as to the values of these loss coefficients. A lot of research is being done in the area of HVAC for the prediction of pressure losses Gan G & Riffat S.B. (1999), Dickey P.S & Cohan J.R (1942)). The improvements in computer simulation packages (CFD) made it easier for researchers to employ numerical techniques to investigate the flow profile and their effects on these pressure loss coefficients. The accuracy of CFD in predicting the pressure loss coefficient has been a subject of great interest to a number of researchers. L. Shao and S.B Riffat (1995) who examined the effects of CFD accuracy of factors including turbulence models, numerical schemes, grid density and domain-set up. They used the CFD package FLUENT to predict pressure loss in a common type of duct fitting i.e., double elbows and found that a combination of k- ϵ model and the higher order QUICK scheme produces the highest accuracy (with a relative error of 10% or less). The grid independency tests they performed showed that a relatively low grid density in the straight upstream and downstream sections of the duct fitting is sufficient but a higher density is required in the section that contained the fitting. S.B Riffat and G. Gan (1997) employed CFD to predict the pressure loss coefficient for rectangular and flat-oval duct

elbows. The CFD results were compared with experimental data from the literature and found to be in good agreement.

The characteristics of different types of dampers like circular, flat plate were previously studied by a number of investigators. Dickey and Coplen (1942) studied pressure losses for flat damper blades with clearance between blades and ducts of about 0.25% of the duct width, which were used for controlling air and gas flow in furnaces. Legg (1986) determined inherent characteristics of single and multi-blade dampers for ducted air systems in terms of the pressure loss coefficient at the fully open position to the loss coefficient at any position blade angle. The pressure loss coefficient across the damper was determined using an insertion loss technique. This technique involved using the pressure difference across two pressure taps upstream and downstream of the damper to calculate the pressure loss due to the damper, taking into account the clear unobstructed duct friction pressure loss. It was found that there was a linear relationship between the logarithm of the loss coefficient and the blade angle. Gan G and Riffat S.B (1999) determined the pressure loss coefficient of square duct with flat plate damper. The CFD package FLUENT and a combination of the standard k- ϵ turbulence model with QUICK difference scheme was used. They also determined the pressure coefficient values experimentally and compared to the CFD results and obtained reasonable agreement.

The pressure loss in ducts is typically characterized by the pressure loss coefficients K . The pressure loss coefficients for duct fittings are tabulated in handbooks by ASHRAE (American Society of Heating, Refrigerating and Air Conditioning Engineers), CIBSE (Chartered Institution of Building Services Engineers) and by many other authors.

Idelchik tabulated loss coefficients for a wide range of pipe fittings, dampers, etc. in the Handbook of Hydraulic Resistance (1986). The coefficients given in the handbook were based on either theoretical formulas or experimental data. The Chapter 9 of Idelchik Handbook of Hydraulic Resistance (1986) contains the pressure loss coefficients across a butterfly valve at different flow velocities and valve openings. The Building services engineering (2001) compiled a guide to the choice of pressure loss coefficients for ductwork components. In this, a survey was undertaken of available data on pressure loss factors of fittings. This paper detailed some of the contradictory information concerning components of ductwork. No CFD work has been presented in the literature so far about the K factor calculations for dampers in circular ducts, and it was found that this current research effort could fill this knowledge gap.

CHAPTER 2

INTRODUCTION AND BACKGROUND

2.1 Background

2.1.1 Dampers

A damper is a mechanical device for controlling the flow of fluids in pipe or any other enclosure depending on the demand for cooling, heating in a space or the flow demands. The control is obtained by a movable element that changes the angle of its blades and therefore the area of its flow passage. In HVAC, dampers regulate the flow of air inside a duct, Variable Air Volume (VAV) box, air handler or any other air handling equipment. They can cut the conditioned air to an unused room or regulate it for room by room temperature and humidity controls.

2.1.2 Damper Actuator

Damper actuators position the dampers according to the signal from the controller. They can be classified as either electric or pneumatic. The electric damper actuators are either driven by electric motors in reversible directions or are unidirectional and spring returned. A reversible electric actuator is used more often for more precise control. The pneumatic activator consists of an actuator chamber whose bottom is made of a flexible diaphragm or bellows connected with the damper stem. When the air pressure in the chamber increases, the downward force overcomes the spring compression and pushes

the diaphragm downward closing the damper and similarly opens it. The pneumatic damper actuator is powerful, simple and reliable.

2.1.3 Types of Dampers

The dampers used in HVAC systems are divided into volume control dampers and fire dampers.

2.1.3.1 Volume Control Dampers

The volume control dampers are classified based on their construction as single-blade dampers or multi-blade dampers. The various types of volume control dampers are:

- Butterfly Damper:

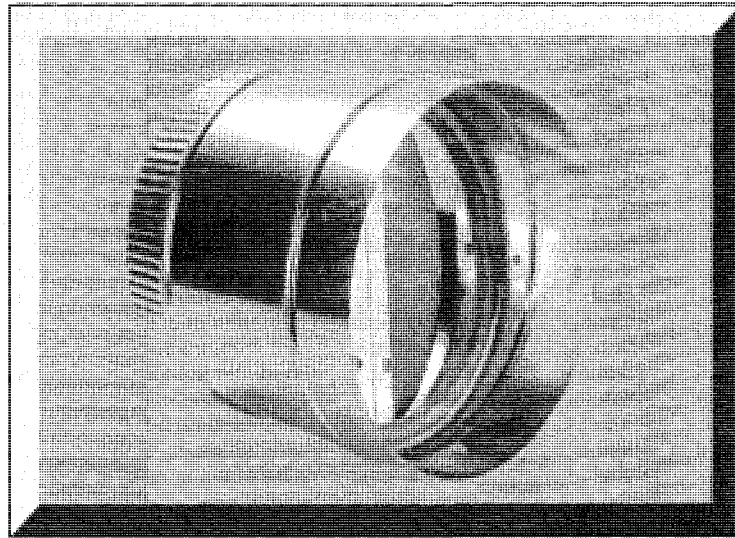


Figure 2 - 1 Butterfly Damper (source www.famcomfg.com/images/BD.gif)

A butterfly damper is a single-blade damper pivoted on a central axle, for a round or rectangular duct. They can be either a low quality and cost shop-fabricated piece of sheet metal with a high leakage rate when closed or a high quality and cost manufactured

damper and frame with practically no leakage when fully closed. This type of damper is mostly used for balancing where tight shut off is not required; hence the shop-fabricated type usually predominates. Figure 2 - 1 shows a butterfly damper.

- Gate Damper:

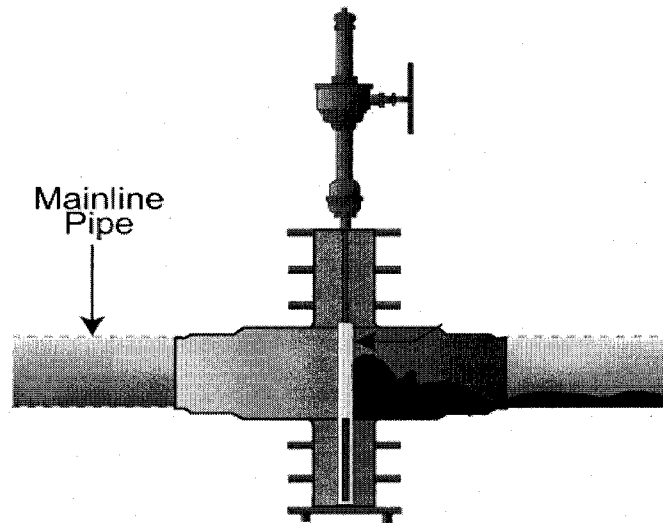


Figure 2 - 2 Gate Damper (source tapseis.anl.gov/.../Gate_Valve_Diagram.jpg)

Gate damper (Figure 2 - 2) is a single-blade damper either rectangular or round in shape. It slides in and out of a slit to shut off or open a flow passage. When open the damper is completely out of the flow stream, and when closed, there is very little leakage. They are mainly used in industrial exhaust systems which handle particulates and with high static pressures.

- Split Damper:

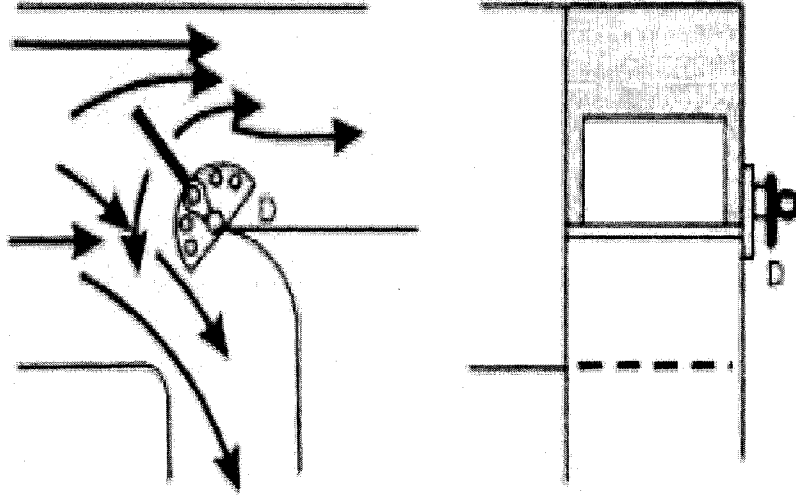


Figure 2 - 3 Split Damper

A split damper shown in Figure 2 - 3, is a single-blade damper, used mainly for balancing at Y junctions. The movement of the damper from one end to the other varies the volume flow of air into the two branches.

- Louver Damper:

A louver damper, a multi-blade damper is a series of center pivoted blades with edges mating in the closed position. It is mostly used for controlling inlet and exhaust flow because it provides more precise control. They are two types of louver damper:

- Parallel-blade damper.



Figure 2 - 4 Parallel Blade Dampers

In the parallel blade dampers, the blades are arranged to rotate in the same direction. They cause high turbulence and hence better mixing, hence perform well for ventilation applications. A parallel blade damper is shown in Figure 2 - 4.

- Opposed-blade damper:

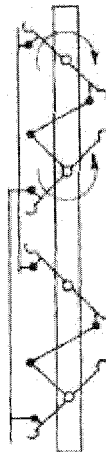


Figure 2 - 5 Opposed Blade Dampers

The opposed blade dampers (Figure 2 - 5) are designed so that the alternate blades rotate in opposite directions. They are preferred for modulating control and are hence intended for variable volume applications such as zone or individual room control.

The multi blade dampers are available with standard (relatively high) or low leakage rates.

2.1.3.2 Fire Dampers

Fire dampers are employed in the fire control strategy. They are fitted where ductwork passes through fire compartment walls. In normal circumstances, the fire dampers are in open position, held by means of fusible links. When there is a fire, these links fracture due to the heat and allow the damper to close under the influence of the integral closing spring.

2.1.4 Damper Sizing

The following procedure is generally employed for sizing of volume control dampers.
[Shan K. Wang, Handbook of Air Conditioning and Refrigeration]

1. The total pressure of the air flow path across the damper is estimated first.
2. The face velocity of the damper is calculated from the obtained pressure loss across it.
3. Depending upon whether the damper is at the entrance, exit, or middle of the flow path, and on the area ratio A_{DAM}/A_d , the local loss coefficient C_{dam} , the face area of the damper is calculated. The area ratio is usually between 0.5 and 0.9.

2.1.5 Damper Losses

The pressure losses due to the operation of the damper are the losses which occur across the damper and the leakage of air through the damper.

2.1.5.1 Pressure Losses

When a fluid flowing steadily in a long straight duct of uniform diameter encounters an obstruction which changes the direction of the whole stream or even part of it, the flow pattern is altered and turbulence is created, causing an energy loss greater than that normally accompanying flow in a straight duct. Since dampers in a duct network disturb the flow pattern they produce additional pressure drop. This loss of pressure by the damper consists of:

- the pressure drop within the damper itself.
- the pressure drop in the upstream piping in excess of that which would normally occur if there were no damper in the duct.
- the pressure drop in downstream duct in excess of that would normally occur if there were no valve in the line; this effect may be comparatively large.

The pressure drop across a fully open damper depends on: damper construction, blade shape, damper dimensions, frame intrusion into the air stream, and the ratio of the cross sectional area of the fully open damper to that of the duct in which it is fixed. [Jones W.P., Air Conditioning Engineering, Fourth Edition]

The pressure loss across the damper is characterized by the pressure loss coefficient k given by the expression

$$k = \frac{\Delta P}{\frac{1}{2} \rho V^2} \quad 1$$

where, k is the pressure loss coefficient

ΔP is the static pressure loss due to damper, Pascals

ρ is the density of air, kg/m³

V is the mean velocity of the air in the duct, m/s

2.1.5.2 Damper Leakage

For the most economical operations, dampers must only allow the amount of air flow as specified by the system and local codes. If dampers do not close tightly the extra air that leaks into the system must be conditioned which requires additional energy. Newer dampers have special seals and friction bearings to reduce leakage. Damper leakage is expressed in two ways: percentage of the air flow per minute per square foot or cubic feet of air per minute per square foot of damper area, both at specified pressure differential.

2.1.6 Applications of Dampers

Dampers are made in different sizes and shapes for installation in round or rectangular ducts. In individual ducts they are used for control of air volume. For diverting or mixing action, two dampers are installed with synchronous operation in two-branch ducts. The simultaneous control of return air and outdoor air in ventilation control is an example of this application. Another important application of dampers is the control of combustion air in burner system.

2.1.7 Building Automation Systems

Building Automation Systems (BAS) are energy management systems which efficiently control the air-conditioning and heating systems. In the BAS, the mechanical

and electrical systems and equipment are joined with microprocessors that communicate with each other and possibly to a computer. The building automation systems, with their efficient operation will become prominent in the future and would replace older and less efficient systems.

The building automation control loop, in order to function efficiently consists of the following:

- Sensor: The sensor measures a medium or monitors the HVAC systems and sends a signal to the control loop.
- DDC: The DDC or the building automation controller holds the program and processes the signal sent by the sensor. In this step, the DDC processed the information sent by the input device and based on the algorithm, sends an output signal to a device to take appropriate action if necessary.
- Controlling device: In this step the controlled device is acting accordingly based on the program variables. Typical output devices can be damper actuators, valve actuators, variable frequency or speed drives etc.

2.2 Significance of the Research

Pressure losses in the duct system of an air handler unit as part of an HVAC system can greatly reduce its efficiency and also increase the cost of energy consumed. The room air distribution in the HVAC system is very important as it essentially influences the room airflow of ventilated and air-conditioned rooms. A wrong design of the ventilation components can lead to uncomfortable draft air as well as excessive energy demand. The accurate knowledge of pressure loss for ducts is crucial for correct plant sizing and

energy efficiency. Owing to its importance in various fluid delivery systems, extensive investigations have been carried out into the flow performance of ducts. Despite the considerable amount of work on k -factors, inconsistencies in pressure loss data still exist. Until recently, experimental measurement was the only way for determining pressure loss coefficient of dampers. The experimental methods were quite useful but were limited to the available fittings. Usually the duct and the damper tested experimentally may not have the same dimensions as the ones practically used, so there would be substantial differences in pressure loss characteristics can occur for the same type of damper. In addition, experimental determination of k -factors is expensive, laborious and time consuming. Recently due to the development of computers and CFD the prediction of pressure losses for any kind of configuration has become possible in a most economical and accurate way.

The predictions of the pressure loss coefficients are useful in the automation of the HVAC system. The knowledge of the pressure losses across the damper can be used as a signal to the pressure transducer which in turn controls the position of the valve. This gives a better control on the HVAC systems which results in less energy losses and higher efficiency.

The objectives of the research are

1. To carry out numerical simulations of circular duct with a circular damper to generate flow profiles and to find pressure loss coefficient.
2. To simulate models with varied flow areas and compare the pressure losses in each case.

The objectives will be achieved by incorporating the following steps

1. Developed a model and discretized into number of elements using HYPERMESH.
2. Used CFD based analysis code to carry on numerical simulations on the discretized model.

CHAPTER 3

NUMERICAL MODELING OF DAMPER

This chapter provides an overview about computational fluid dynamics (CFD), the CFD simulation software Star-CD and the model used for the process.

3.1 Computational Fluid Dynamics

Computational Fluid Dynamics (CFD) is that branch of fluid mechanics which solves fluid flow problems employing numerical methods and algorithms. Computers are used to simulate the interaction between fluids and gases with the surface and perform the calculations. The Navier-Stokes equation which is the fundamental equation of fluid and which defines any one phase fluid flow problem is the basis for CFD. When the flow is inviscid, the viscosity terms in the Navier-Stokes equation are dropped to obtain Euler's equation. The capability of CFD to solve any complex contours makes it used for the study of wide range of problems involving fluid flow. In summary, CFD can be used for component modeling, system analysis, design verification and optimization. Some of the commercial CFD codes available are Star-CD, Fluent, Proflow, etc.

One of the general methods to work in CFD is to discretize the given flow problem and solve the equations of motion by using a suitable algorithm. The basic procedure usually followed is the same.

1. Preprocessing

- geometry of the model defined.
- problem discretized to finite elements
- description of the physical model
- defining the boundary conditions

2. Simulation. The simulation is started by specifying the number of iterations and other solution parameters.

3. Postprocessing. The results obtained from the simulations are analyzed and visualized as the interpreter desires.

The significant methods of discretizing a model are Finite Volume Method, Finite Element Method and Finite Difference Method. A brief insight is given on the finite volume method which is the one typically used in CFD codes.

Finite Volume Method

The Finite Volume Method is one of the versatile methods used in CFD. The governing equations are solved on control volumes. This method rearranges the partial differential equations of Navier–Stokes equations in conservative form and then discretizes these equations. In this method the first step is to divide total domain into number of control volumes where the variable of interest is located at the centroid of the control volume. The next step is to integrate the differential form of the equations over each control volume. The resulting equation is known as the discretization equation.

The important feature of the Finite Volume Method is that the resulting solution satisfies the conservation of quantities such as mass, energy, momentum. This is satisfied for every control volume and hence for the whole domain. Even for a coarse grid the solution satisfies the exact integral balance.

Finite Volume Method is ideal solution for compressible flows where discontinuous solutions are there. Any discontinuity in flow must satisfy Rankine-Hugoniot condition which is developed from conservation law. As Finite Volume Method is conservative it obviously satisfies Rankine-Hugoniot condition.

3.2 Star-CD

Star-CD is the commercially available CFD software which employs the finite volume method in its solution algorithm. It is known for being the most versatile platform for industrial CFD simulations. It is capable of simulating problems involving turbulence, combustion, heat transfer, reactions and multiphase physics. Star-CD can import a model from any CAE tool and generate a computational mesh and simulate it. Star-CD consists of three modules Prosurf, Proam and Prostar.

3.2.1 Prosurf

Prosurf is a stand-alone program which can read CAD data saved into one of several supported formats, repair common CAD errors either automatically or manually and triangulate the surface for further use by pro-am or other volume meshing programs. This tool simplifies the process of converting CAD surface and curve data into surface mesh which captures all the features and resolves various geometric shapes. Many of the

tedious CAD repair operations are automated, thereby reducing the time and effort required to obtain a complete and closed surface geometry with no defects.

3.2.2 Proam

Proam or Prostar automesh module provides various tools needed to generate mesh for any complex engineering problem. It also features additional capabilities such as new surface generation, surface repair and subsurface creation and wide range of other tools for high quality mesh generation. The different types of meshes that can be generated using Proam are trimmed, tetrahedral and hybrid.

3.2.3 Prostar

Prostar is the final module which allows analyzing the given problem. The given model after being processed in Prosurf and Proam is brought into Prostar for running simulations. All the flow parameters such as boundary conditions, the nature of flow and solution method are specified using the available tools. This module also contains tools required for post-processing the obtained simulation results.

3.3 Model Description

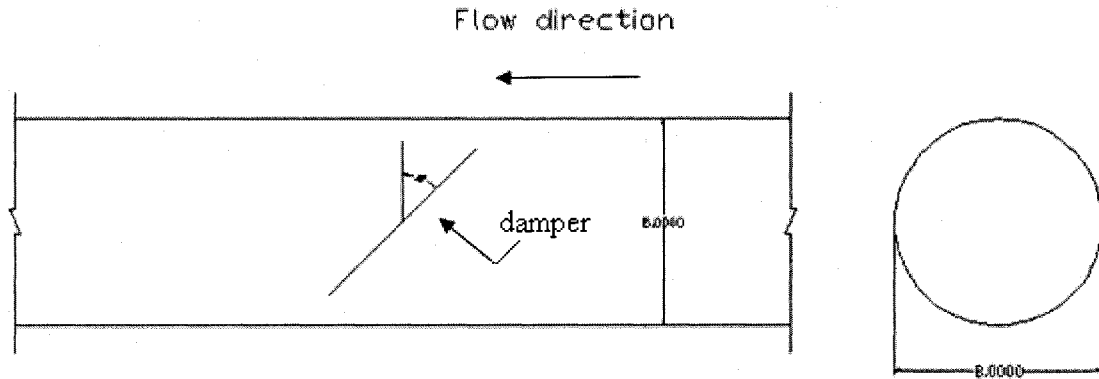


Figure 3 - 1 Schematic of the duct with a single-blade damper

This section discusses about the models created and used for simulation to obtain the pressure loss coefficients of the damper. Figure 3-1 shows the schematic of the circular duct with the damper. The modeling methodology and the specified conditions under which the simulations were performed are also enumerated. The most representative HVAC duct size of 8'' and damper of 1/4'' thickness were chosen for the model. These are the assumptions and boundary conditions used in this model:

- The inner surface of the duct is assumed to be smooth and with no slip conditions.
- The flow is considered to be isothermal (293K) incompressible and turbulent.
- The initial velocity is axial with cross flow components set to zero.
- The molecular properties of the fluid are standard air properties presented in Table 3-1
- The ambient pressure is 0 Pa gauge.

Five different damper positions were considered

1. Damper of thickness $\frac{1}{4}$ " inclined at 15 degrees to the perpendicular to the axis of the duct.
2. Damper of thickness $\frac{1}{4}$ " inclined at 30 degrees to the perpendicular to the axis of the duct.
3. Damper of thickness $\frac{1}{4}$ " inclined at 45 degrees to the perpendicular to the axis of the duct.
4. Damper of thickness $\frac{1}{4}$ " inclined at 60 degrees to the perpendicular to the axis of the duct.
5. Damper of thickness $\frac{1}{4}$ " inclined at 90 degrees to the perpendicular to the axis of the duct.

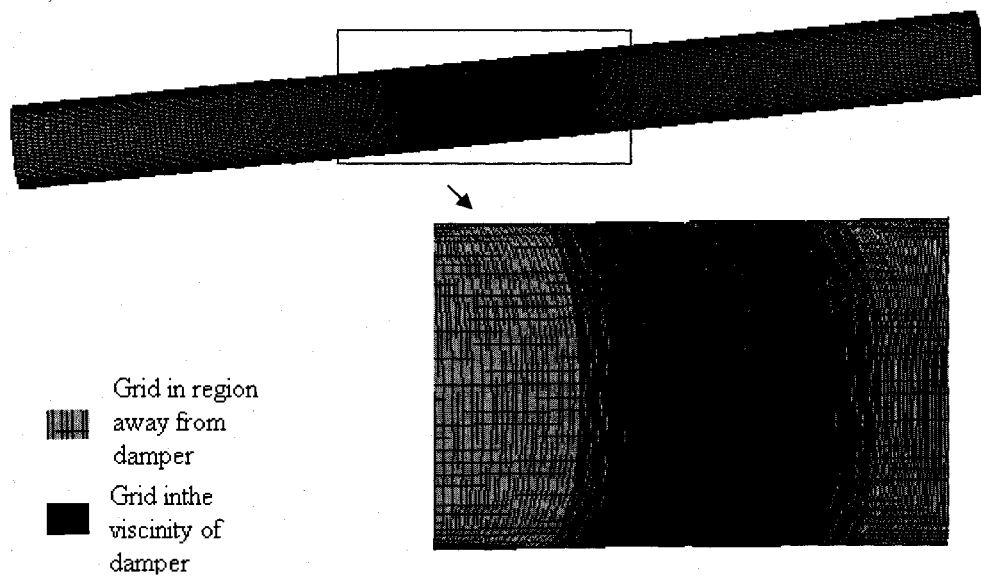


Figure 3 - 2 Model with tetrahedral mesh for simulation

The models geometry was developed using the CAD software Pro-Engineer and imported to meshing software known as Hypermesh. In Hypermesh, a tetrahedral mesh was generated (Figure 3-2). From the figure it is evident that a uniform mesh was not employed all throughout the volume of the duct. The presence of the damper in the midway of the duct would make the flow in that region susceptible to heavy pressure and velocity gradients. Hence a finer mesh was used in the regions surrounding the damper and a course mesh was used in the regions far upstream and downstream of the damper. In this way a better visualization of flow parameters in the regions near to the damper is obtained. The model was imported as a Nastran file to Prostar, where the analysis was performed. The model imported from Hypermesh was checked for any failures using the tools in Prostar.

The duct entrance is defined as inlet boundary condition with velocity of flow (uniform or otherwise) being specified. The outlet is defined as a pressure boundary condition with ambient pressure set to zero gauge. The entire outer surface of the duct corresponds to default wall boundary condition. The molecular properties of air available in the Star database have been used. From the previous studies, it has been found that a combination of the standard k- ϵ high Reynolds numbers turbulence model (Launder and Spalding, 1974) with QUICK difference scheme (Leonard, 1979) produces the best results for pressure distribution in ducts.

Since the flow is considered to be isothermal and incompressible the temperature and buoyancy options are turned off. The steady state analysis with SIMPLE solution algorithm was employed. The solver parameters for velocity, pressure and turbulence were selected based on the convergence of the model. After setting the model and the

parameters in Star-CD the model is run and the obtained results are analyzed using the post-processing module.

Five different values of Reynolds number were used for simulating the models. Reynolds numbers of 0.29×10^5 , 0.44×10^5 , 0.59×10^5 , 0.74×10^5 , and 0.89×10^5 which correspond to inlet velocities of 400 fpm to 1200 fpm, typically found in HVAC systems, were used. The molecular properties used during the simulations are listed in Table 3 - 1. These are the properties of air available in the Star-CD database.

Table 3 - 1 Molecular Properties of Fluid

Density	1.205 kg/m^3
Molecular viscosity	$1.81 \times 10^{-5} \text{ kg/ms}$

Table 3 - 2 Coefficients of the High Reynolds Number k- ϵ Turbulence model

C_μ	$C_{\epsilon 1}$	$C_{\epsilon 2}$	$C_{\epsilon 3}$	$C_{\epsilon 4}$	κ	σ_k	σ_ϵ	σ_h
0.09	1.44	1.92	1.44	-0.33	0.419	1	1.219	0.9

Table 3 - 2 shows the coefficient values of the standard k- ϵ Turbulence model available in Star-CD.

CHAPTER 4

RESULTS AND DISCUSSION

4.1 CFD Simulations

This section presents and discusses the results obtained from the simulations using the CFD package Star-CD.

4.1.1 Grid Independency Results

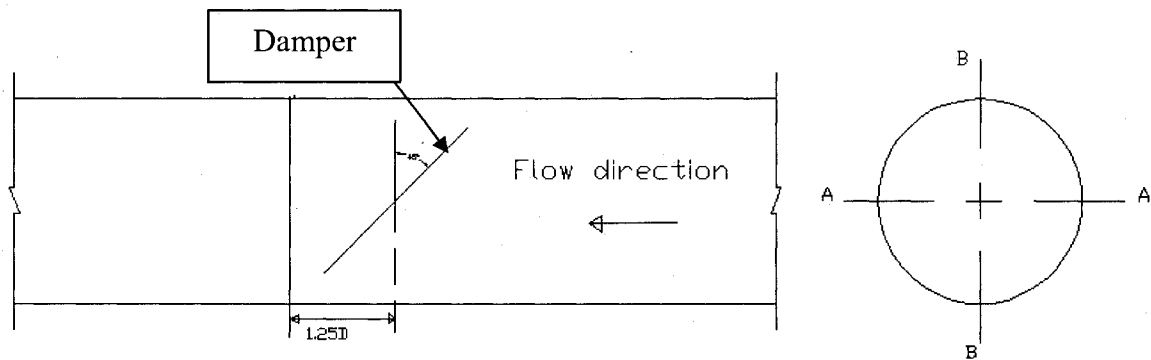


Figure 4 - 1 Cross-section of the duct considered for grid independency test

While performing CFD analysis it is very important to ensure that the grid independency criterion is satisfied for the models. Grid independency is the non variation of the results with change in the grid density. It is performed to make sure that the ideal grid size is used during the computation process which avoids the unnecessary computational space and time. It is one way to make the best use of available resources economically. Due to the similar configuration of the models, the grid independency was performed for the damper at one angle and one Reynolds number. This was done by

increasing the grid size each time and running the simulations. The results obtained from each grid size are compared. The model was said to achieve grid independency when the solutions from two grid sizes are within predetermined tolerance limits, the lower grid density being used for further analysis.

The model with damper angle of 30 degrees and Reynold's number 30000 was used to perform the grid independency tests. The Z-component velocity i.e. velocity parallel to the axis of the duct was tested. A course grid of 100,000 and a fine grid of 600,000 were used. A cross-section 1.25D downstream of the damper (Fig 4-1) was considered for the study and the velocity was plotted along a diameter parallel and normal to the damper axis. Figure 4-2 and 4-3 show the grid independency test results. The average variation in the velocity component in Z direction for grid size of 400000 cells and 600000 cells along a diameter parallel to the axis of the damper is not more than 0.02 % and along a diameter normal to the axis of damper is about 0.003 %. Hence the grid size of 400000 cells is acceptable for the simulations. Figures 4-2 and 4-3 show the grid independency results.

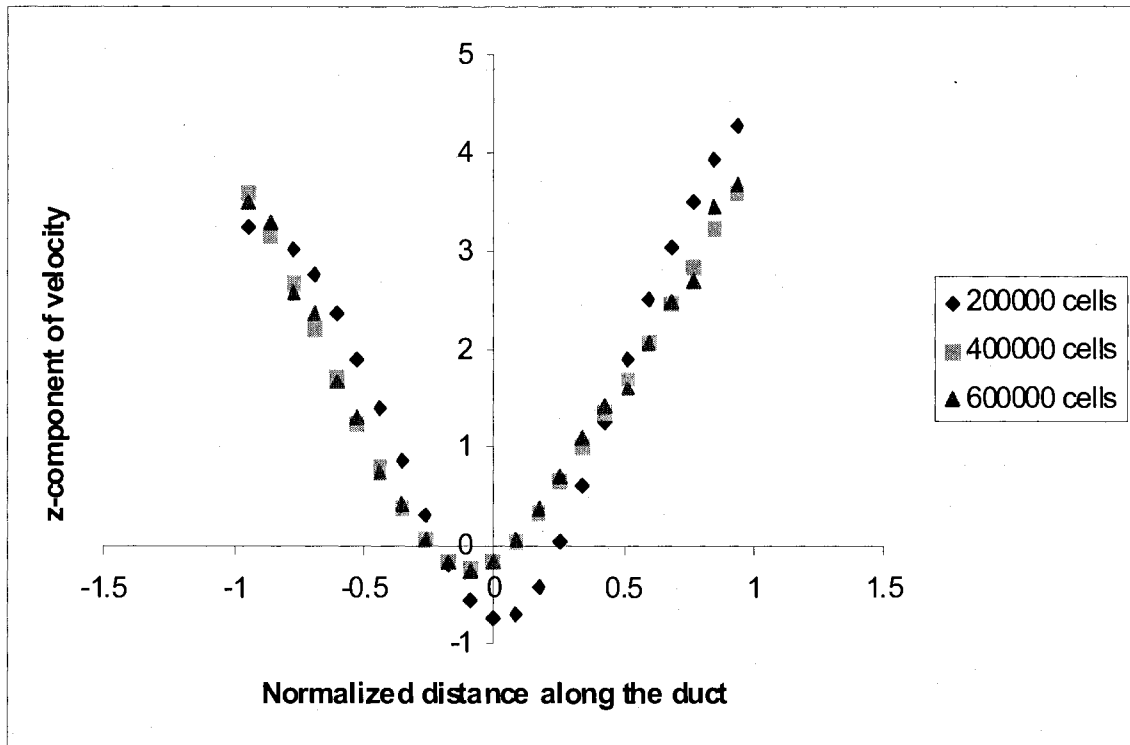


Figure 4 - 2 Z-component of velocity (m/s) along a diameter parallel to the direction of the damper axis

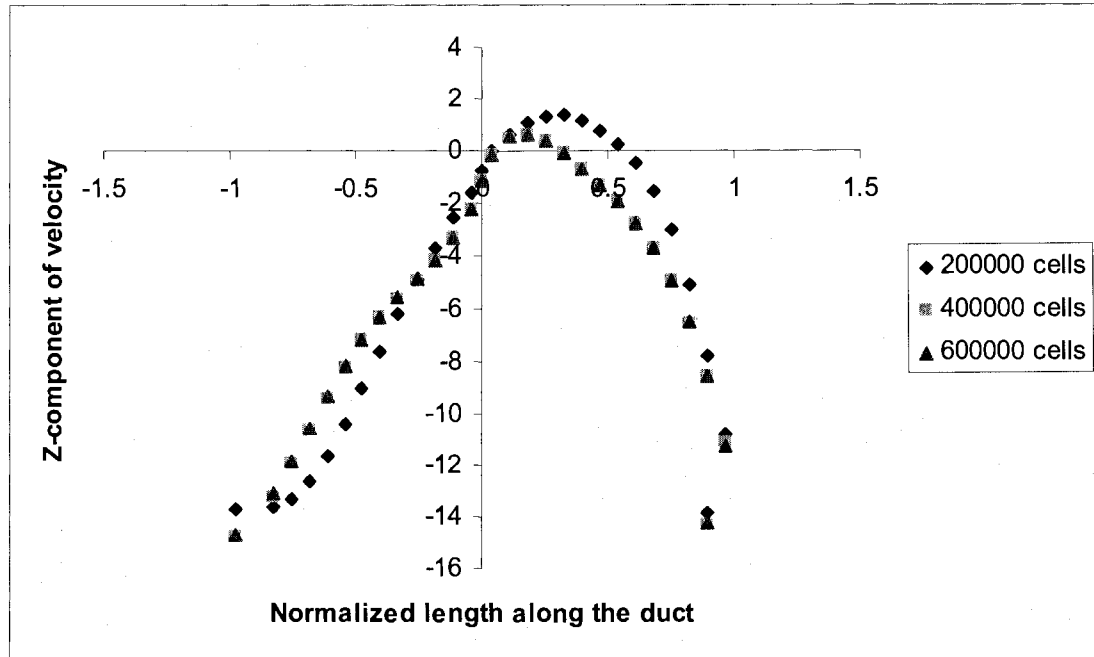


Figure 4 - 3 Z-component of velocity (m/s) along a diameter normal to the direction of the damper axis

4.1.2 CFD Simulation Results

Whenever there is an obstruction to a fluid flow, such as a change in area, a substantial pressure loss occurs. The CFD analysis code Star-CD was used to predict the air flow and pressure distribution in duct with dampers at different angles over a range of Reynolds number. The results of the different models are presented in this section.

Figure 4 - 4 shows the velocity distribution in the duct with the damper held at 30 degree angle with an inlet velocity of 400 fpm ($Re=30,000$). The image in the top of the figure shows the velocity distribution through the entire duct. The area encompassing the damper is enlarged and presented to obtain a better understanding of the velocity profile. The upstream of the damper has uniform velocity as can be seen from the figure. The Figure 4 - 5 shows the extended view of the velocity profile in the region downstream of

the damper. As seen from the figures, because of the presence of the damper, abrupt contractions and expansions occur. All this is associated with local increase in velocities and flow separations result. A recirculation zone is formed in the downstream because of the damper, but the flow in the upstream of the damper is uniform with no disturbances.

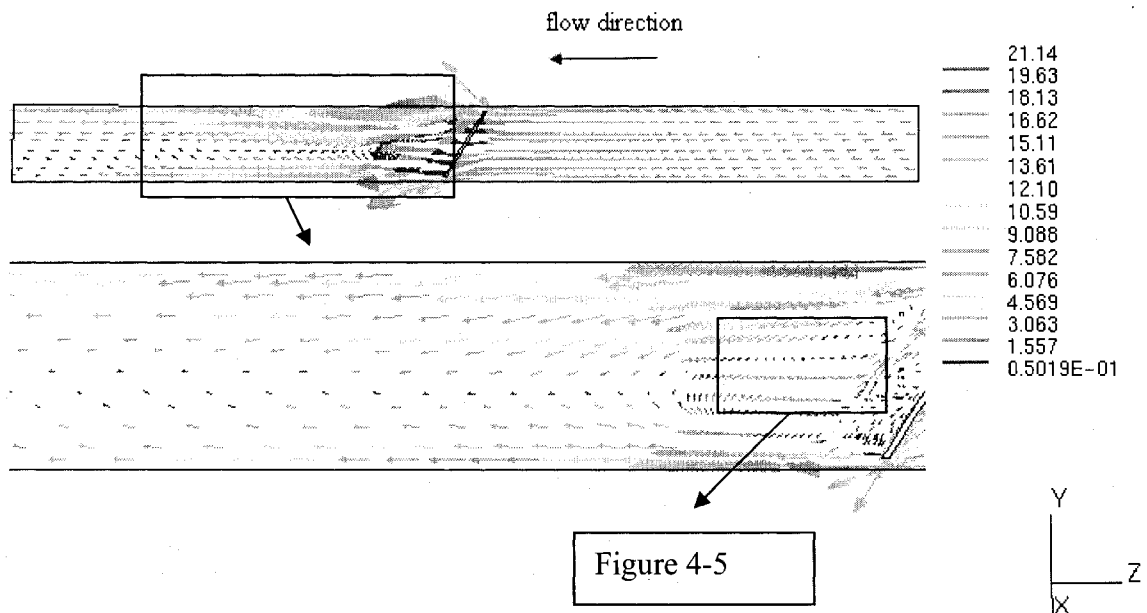


Figure 4 - 4Velocity (m/s) vector plot for 30 degree damper opening at Re=30000

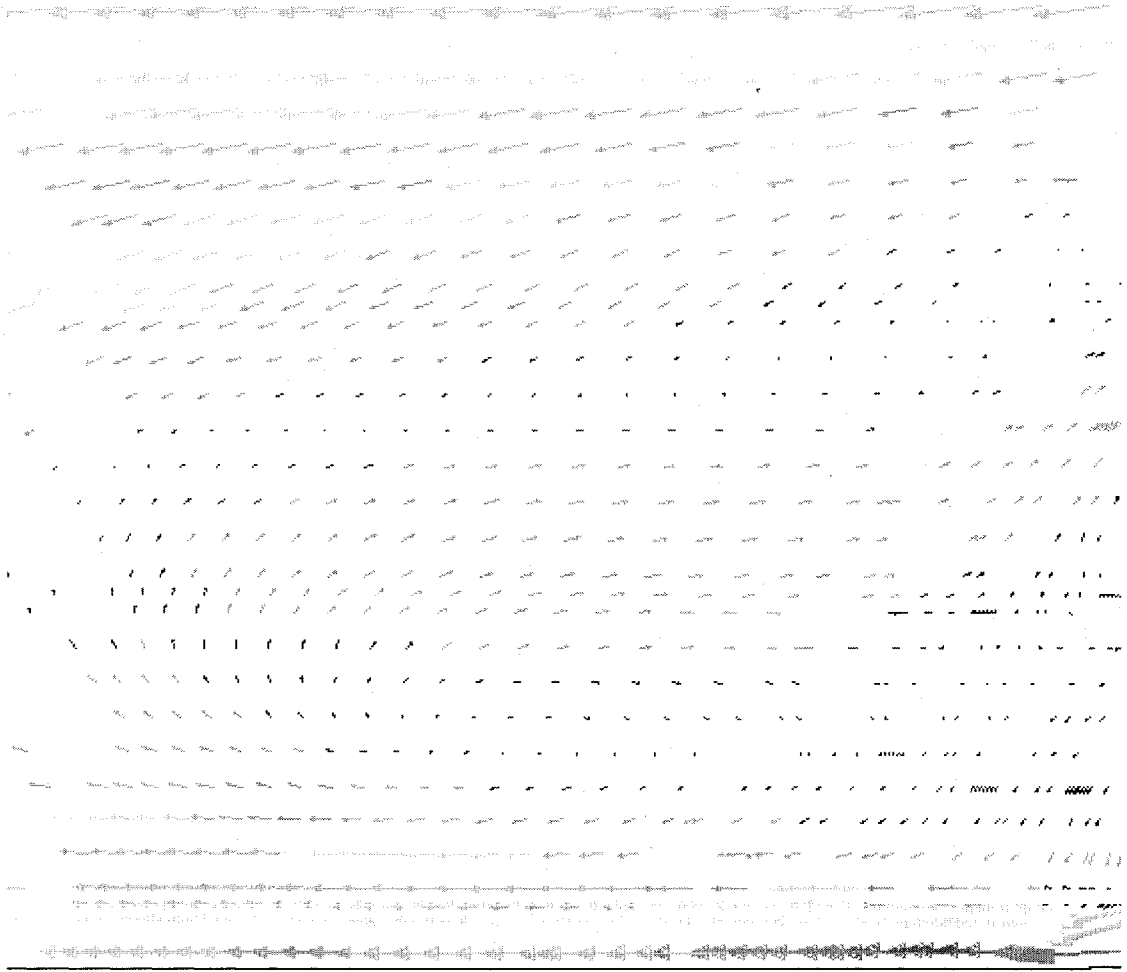


Figure 4 - 5 Velocity (m/s) vector plot downstream of the damper at 30 degree $Re=30000$

The total pressure distribution along the duct is shown in the Figure 4-6. The pressure in the upstream of the damper is uniform. The pressure in the downstream of the damper due to the increased velocities and recirculation falls below the reference pressure which results in negative gauge pressures as can be seen in the figure.

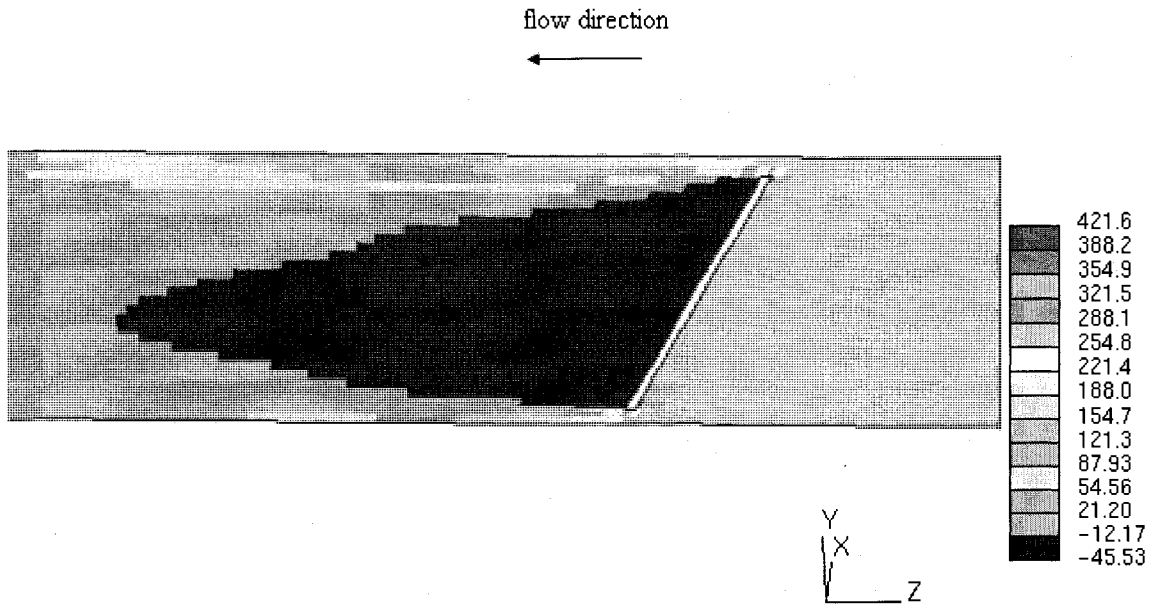


Figure 4 - 6 Pressure (Pa) profile for 30 degree damper opening at $Re=30000$

The flow across the damper was also studied for other Reynolds numbers, while fixing the damper angle at 30 degree. Figures 4-7 and 4-8 show the velocity and pressure profile when the Reynolds number is 45000. Figures 4-9 and 4-10 show the velocity and pressure profile when the Reynolds number is 60000. Figures 4-11 and 4-12 show the velocity and pressure profile when the Reynolds number is 75000. Figures 4-13 and 4-14 show the velocity and pressure profile when the Reynolds number is 90000. As the Reynolds number increases, the magnitude of the velocities and pressure through out the duct increase. This is due to the increased inlet velocities. The strength of the recirculation zone is also increased. The blue regions in the above figures indicate the region of low pressure. These low pressure regions result due to the presence of damper and sudden obstruction to the flow of air.

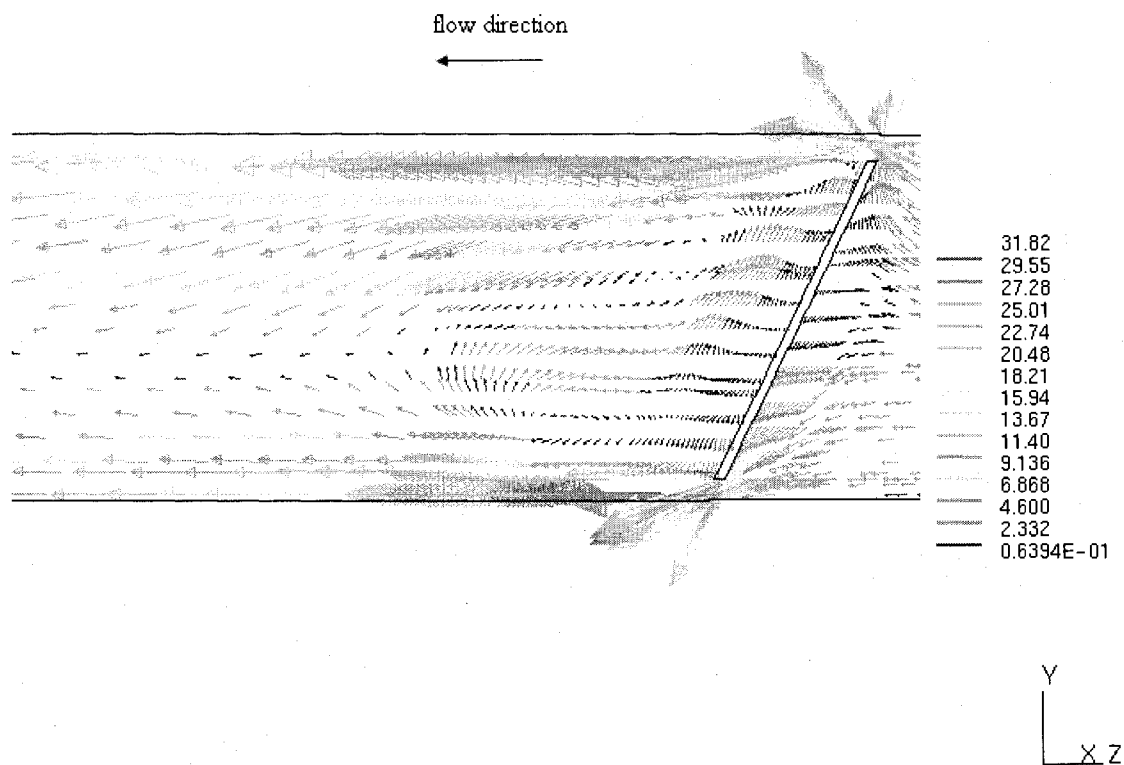


Figure 4 - 7 Velocity (m/s) vector plot for 30 degree damper opening at $Re=45000$

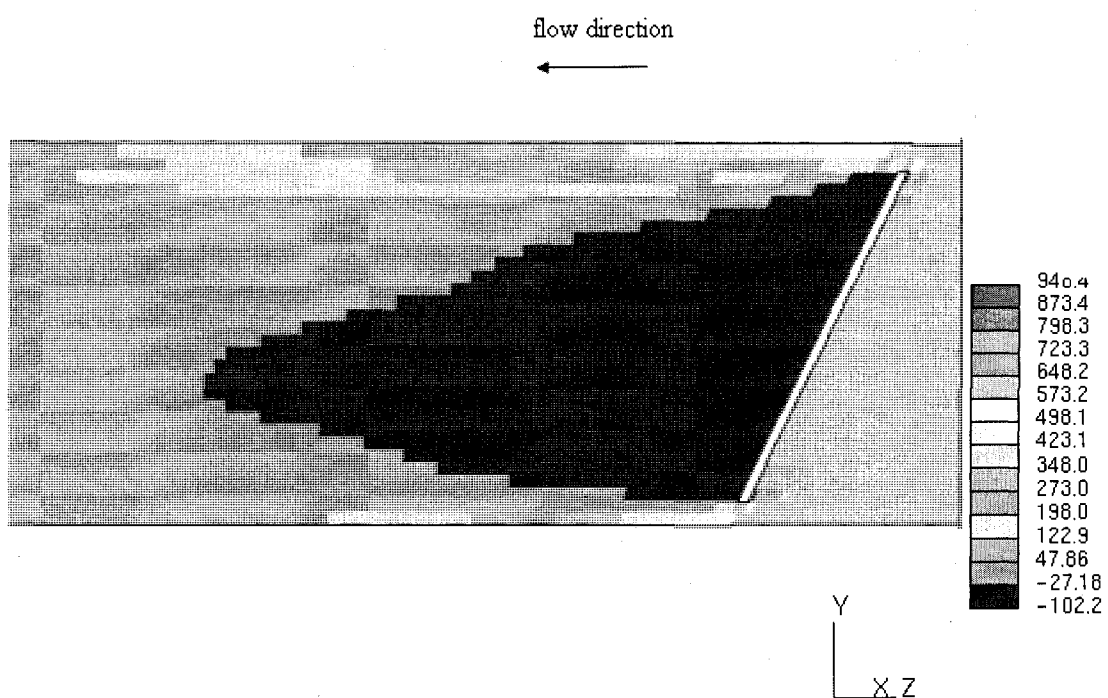


Figure 4 - 8 Pressure (Pa) profile for 30 degree damper opening at $Re=45000$

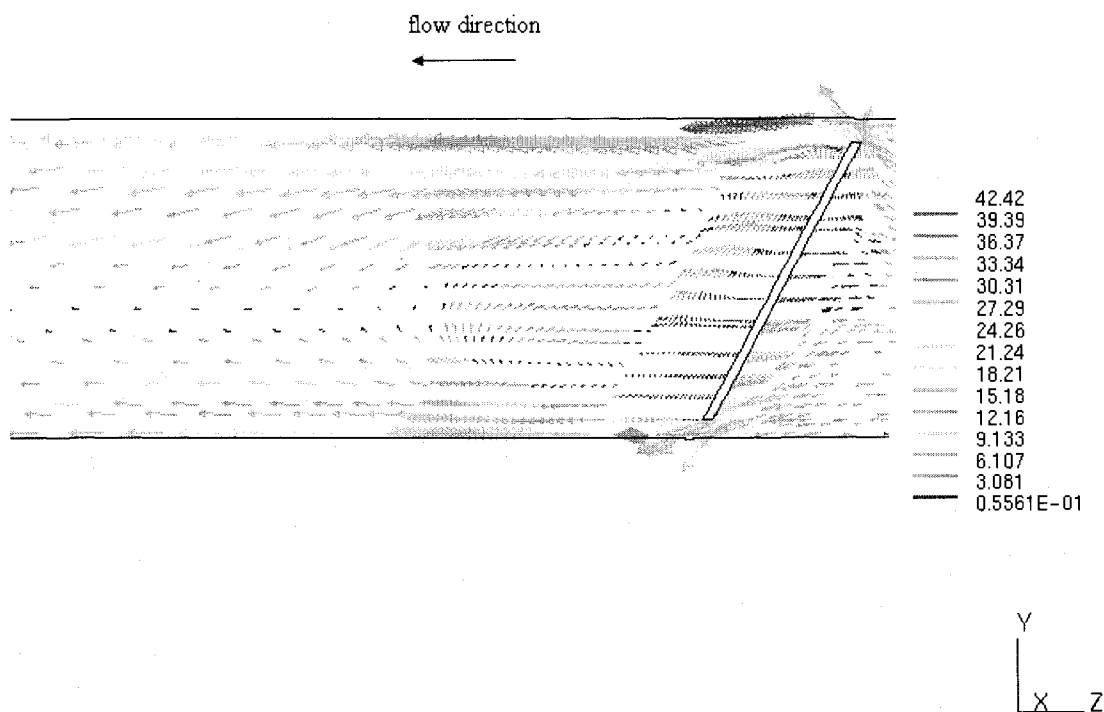


Figure 4 - 9 Velocity (m/s) vector plot for 30 degree damper opening at $Re=60000$

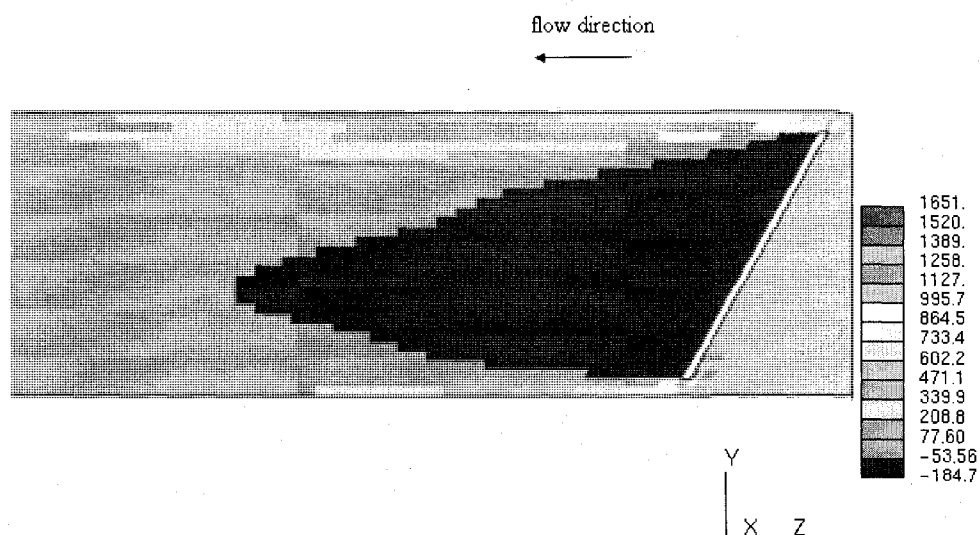


Figure 4 - 10 Pressure (Pa) profile for 30 degree damper opening at $Re=60000$

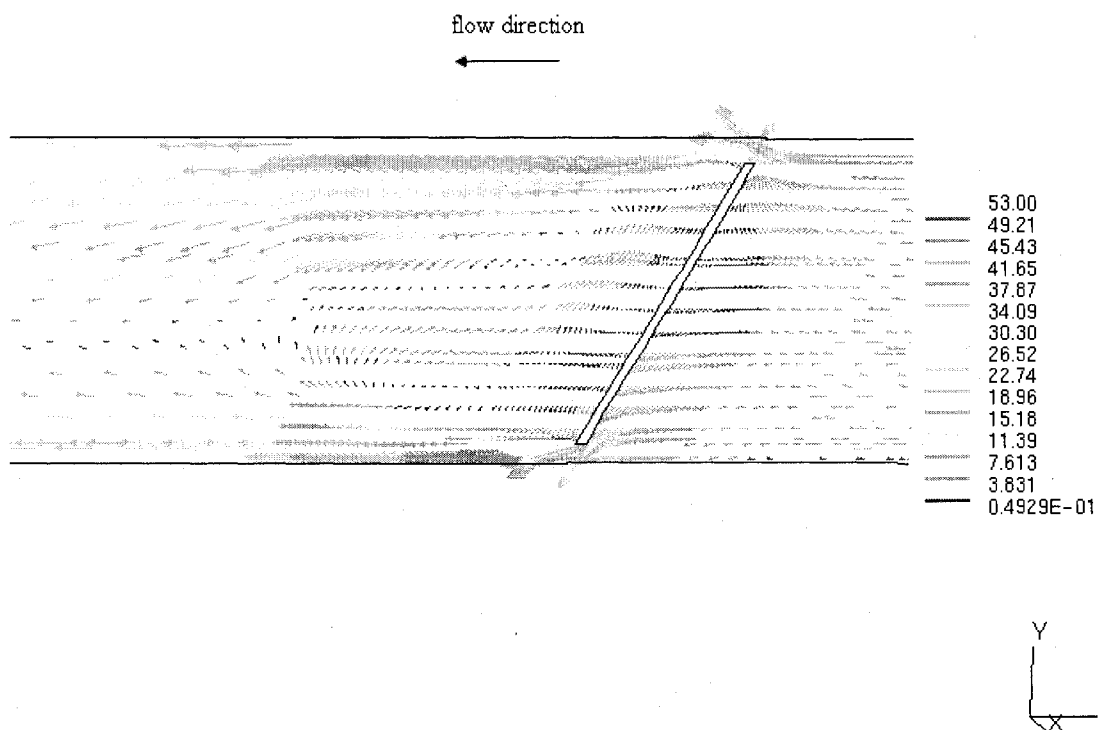


Figure 4 - 11 Velocity (m/s) vector plot for 30 degree damper opening at $Re=75000$

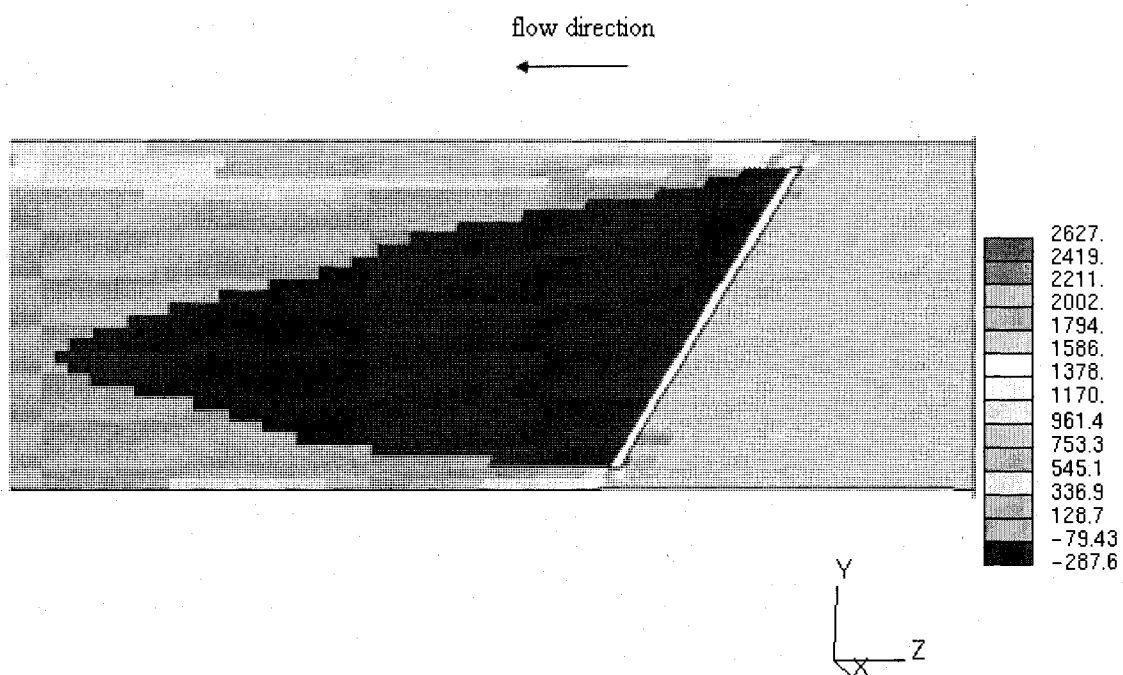


Figure 4 - 12 Pressure (Pa) profile for 30 degree damper opening at $Re=75000$

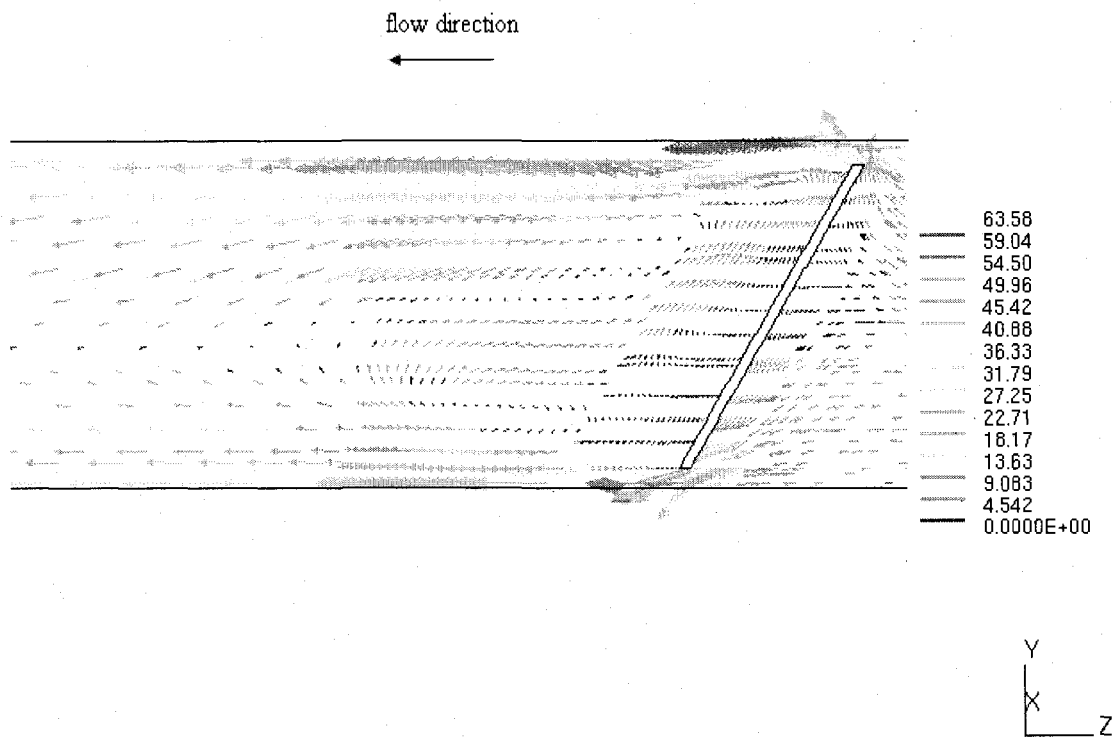


Figure 4 - 13 Velocity (m/s) vector plot for 30 degree damper opening at $Re=90000$

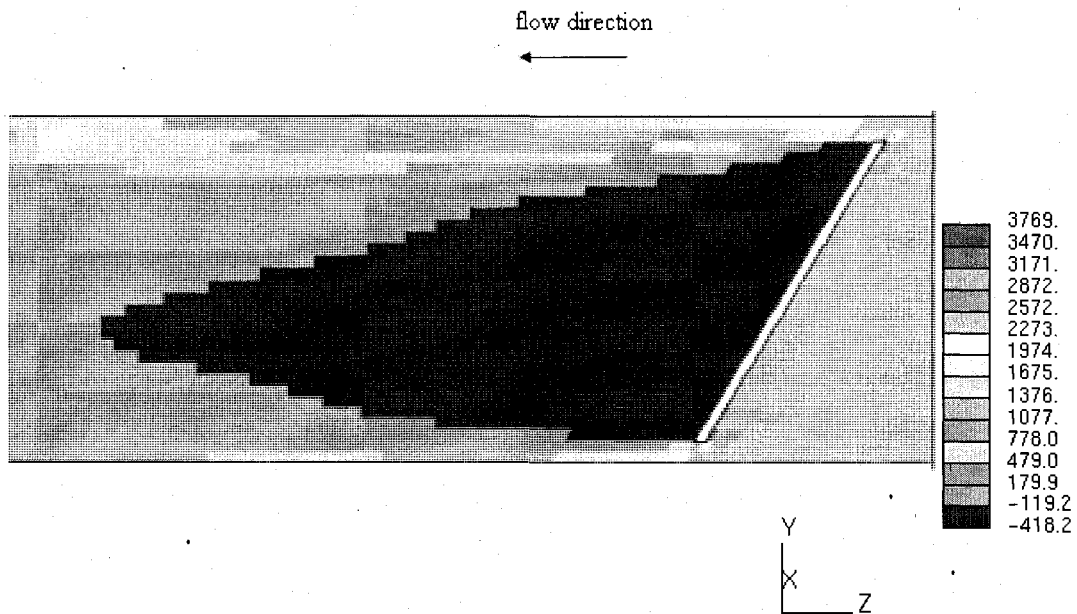


Figure 4 - 14 Pressure (Pa) profile for 30 degree damper opening at $Re=90000$

The variation of static pressure along the length of the duct is shown in Figure 4-15. The average static pressure at each cross-section was calculated as the area average of the static drop of the cells lying at that particular section. A considerable pressure loss can be noticed across the damper location which is the midway of the duct as opposed to the pressure drop along the straight duct. The figure also shows the static pressure distribution along the duct for different Reynolds numbers. As seen from the above velocity and pressure plots, the magnitude of the static pressure distribution along the duct increases with the Reynolds number. The presence of the damper causes a sudden change of the path of the air flow. The air squeezes itself in the small area available on the top and bottom of the damper resulting in higher velocities and sudden pressure drop.

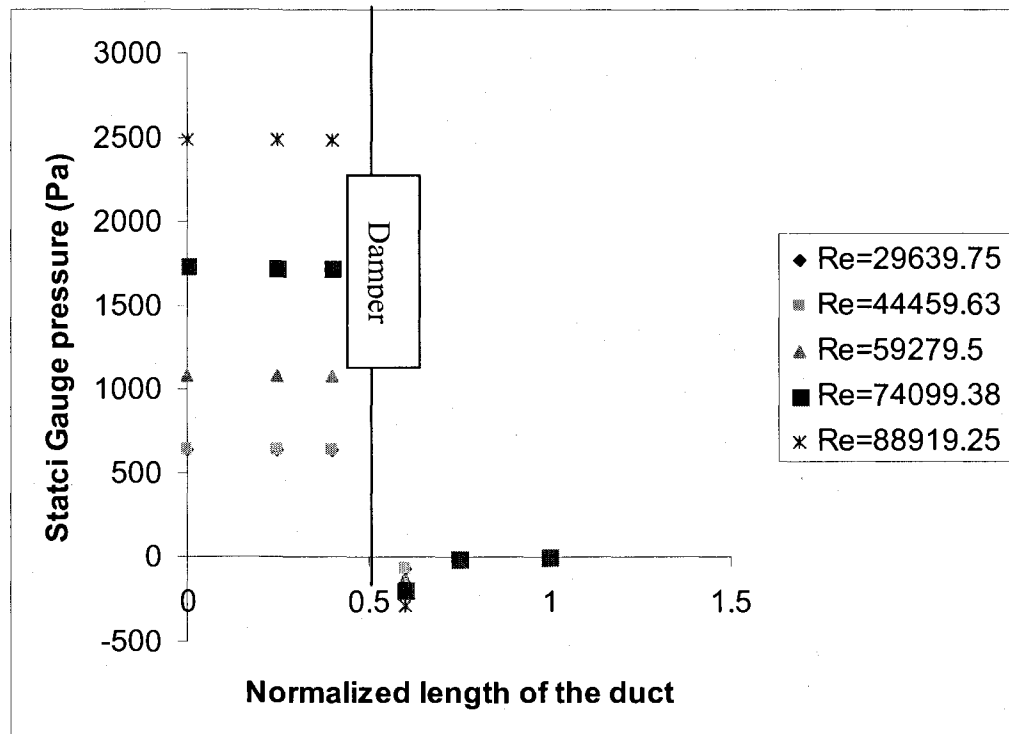


Figure 4 - 15 Gauge static pressure (Pa) along the duct for 30 deg damper angle

The velocity and pressure distribution for 45 degree damper opening at a Reynolds number of 30,000 is shown in Figures 4-16 and 4-17. The velocity and pressure values as seen from the profiles are low when compared to the corresponding 30 degree flow. As the damper angle increases more flow area is available for the air and so the pressure drop is relatively lower than for smaller opening angles. The recirculation zone is decreased as a result of the lower pressure drops.

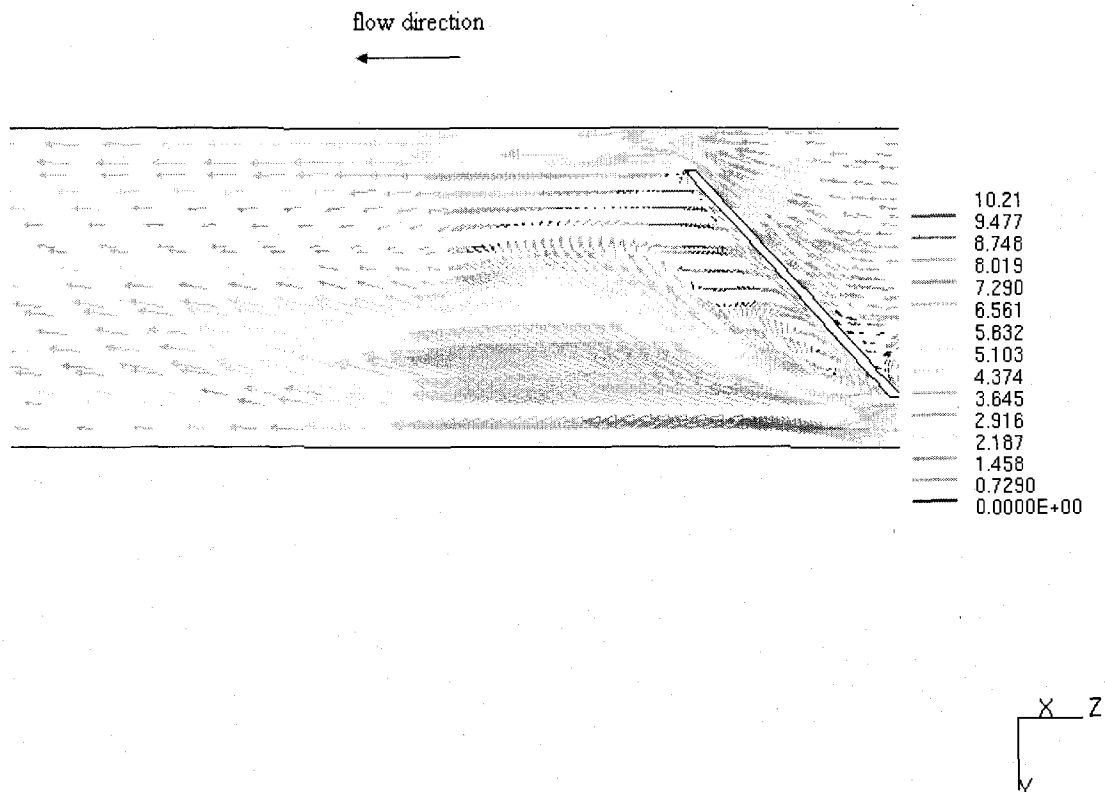


Figure 4 - 16 Velocity (m/s) vector plot for 45 degree damper opening at $Re=30000$

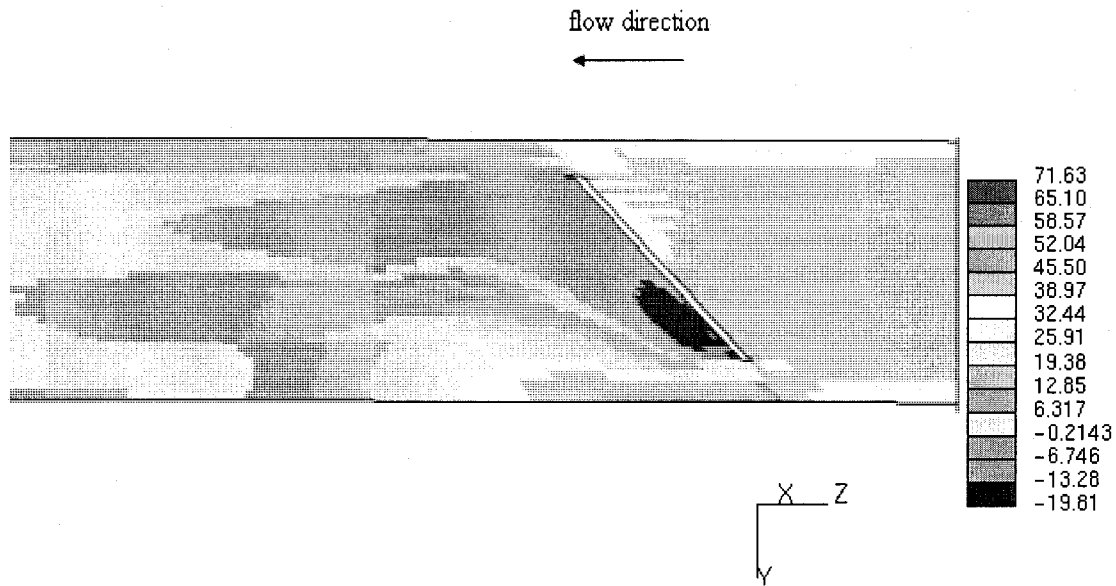


Figure 4 - 17 Pressure (Pa) profile for 45 degree damper opening at $Re=30000$

Figure 4-18 depicts the interesting case when the damper is completely open i.e., 90 degree damper angle. As the damper is a circular plate of $\frac{1}{4}$ " thickness, its surface offers some resistance even when it is fully open. As seen in the figure there is a slight pressure drop across the damper. There is no recirculation zone and separation of flow as the pressure drop is very low.

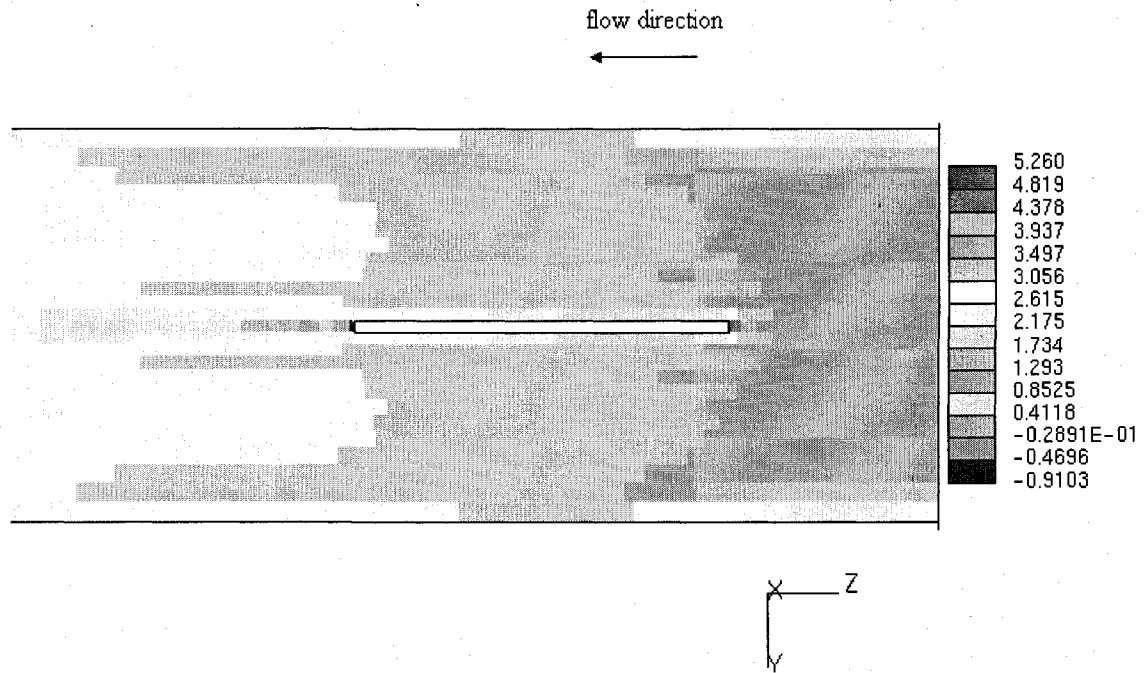


Figure 4 - 18 Pressure (Pa) profile for 90 degree damper opening at $Re=30000$

Figure 4-19 shows the gauge static pressure distribution along the length of the duct for the 15 and 30 degree damper opening. Figure 4-20 shows the gauge static pressure distribution along the length of the duct for the 45 and 90 degree damper opening. The static pressure values are high for the 15 degree damper opening and decrease as the damper angle increases.

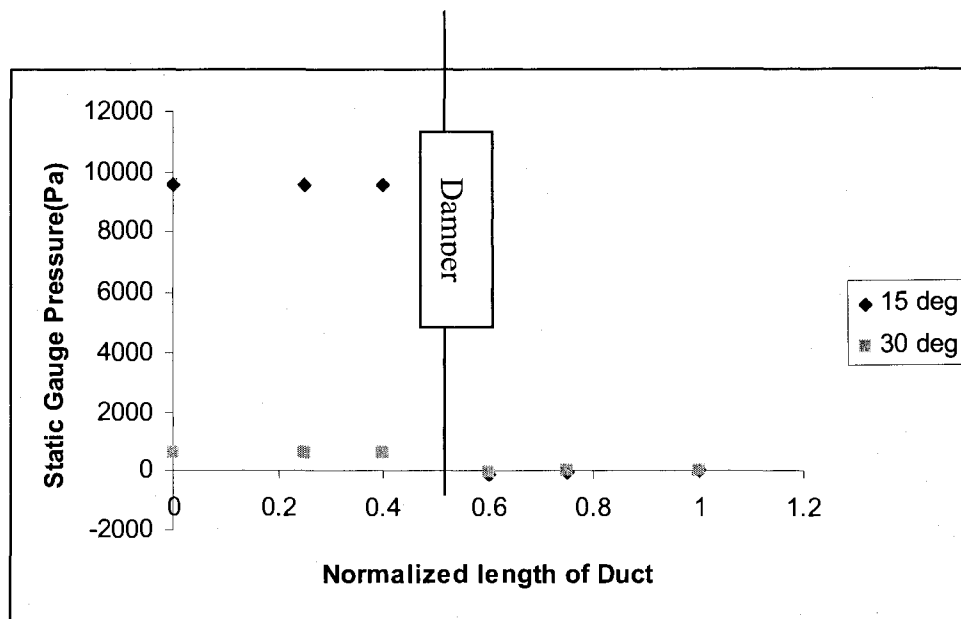


Figure 4 - 19 Static gauge pressure along the duct at 15 & 30 degrees $Re=30000$

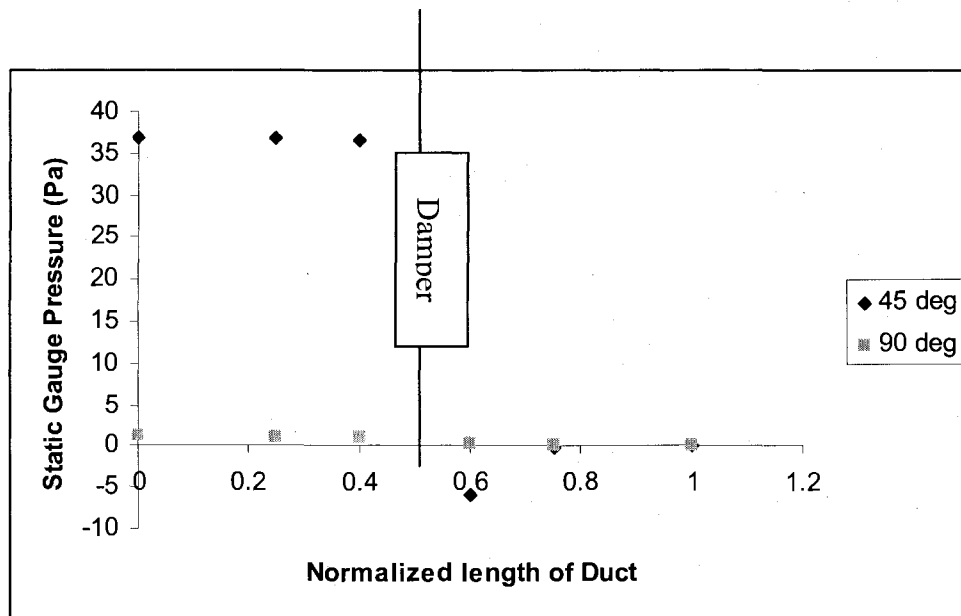


Figure 4 - 20 Static gauge pressure along the duct at 45 & 90 degrees $Re=30000$

4.1.3 Prediction of Pressure Loss Coefficients

The energy loss in the duct due to the damper is characterized by a dimensionless parameter called pressure loss coefficient or k-factor. The k-factor is determined by the equation [1]. The static pressure drop values across the duct are obtained from the plots of the static pressure distribution along the length of the duct. The static pressure values were determined as the average values across the cross section in the upstream and downstream of the damper free from damper interference. Then the values were plotted all along the duct and the values were taken in the region downstream and upstream of the damper. This was the general procedure employed by the other researchers (Gan G., Riffat S.B. 1999) to predict the pressure loss coefficient. The static pressure readings 2D upstream and downstream of the damper were taken to determine the static pressure loss across the damper. The density of the air is 1.205 kg/m^3 . The values of the k-factors are determined by the above process for all the five damper positions and 5 Reynolds numbers.

The values of the k-factors obtained were compared to those of Handbook of Hydraulic Resistance, Idelchik (1986) for a circular geometry duct and with those of published paper by Gan G, and Riffat S.B. (1999) which are for a square duct. Figure 4-21 shows the predicted values and values obtained from Idelchik (1986) for damper angles of 15 and 30 degrees. The values for 45, 60 and 90 degrees are shown in Fig 4-22. The predicted values are in general good agreement with the Idelchik I.E (1986) values. The difference is slightly pronounced at smaller angles. As the damper angle increases the difference in the values decreased. The values in the handbook are determined using a few analytical tools. The construction of the damper in the study by Idelchik was similar

to the one studied for this research. The only difference being the thickness of the damper not being specified by Idelchik. As the thickness of the damper effects the air distribution in the duct, there might a slight difference due to this fact. The difference in the values can also be attributed to the fact that the real nature of flow would be different to that of the theoretically analyzed one.

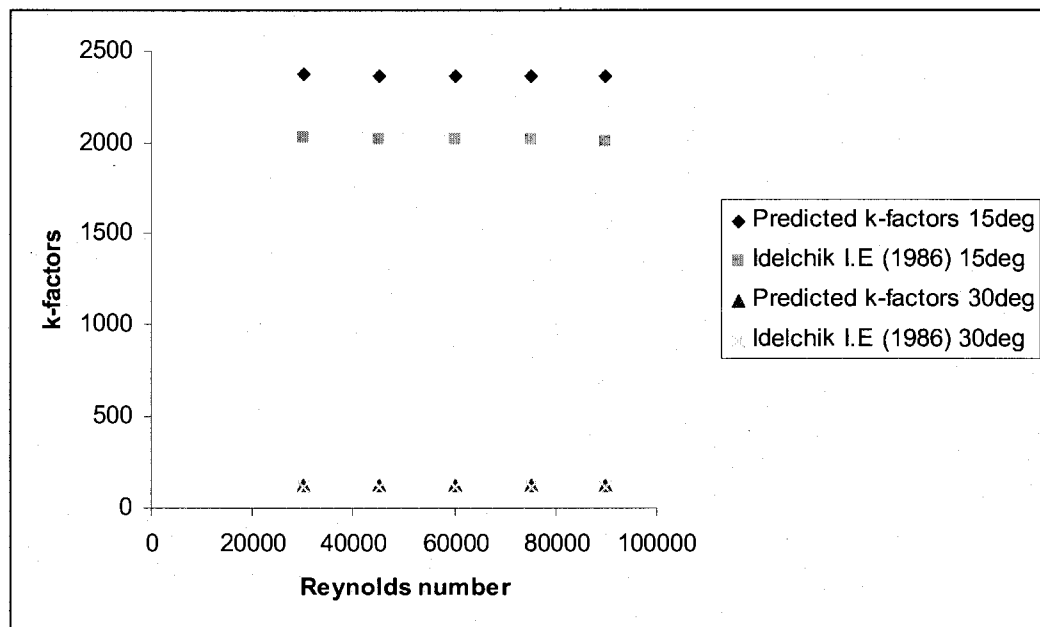


Figure 4 - 21 Comparison of k-factors at 15 and 30 deg damper opening

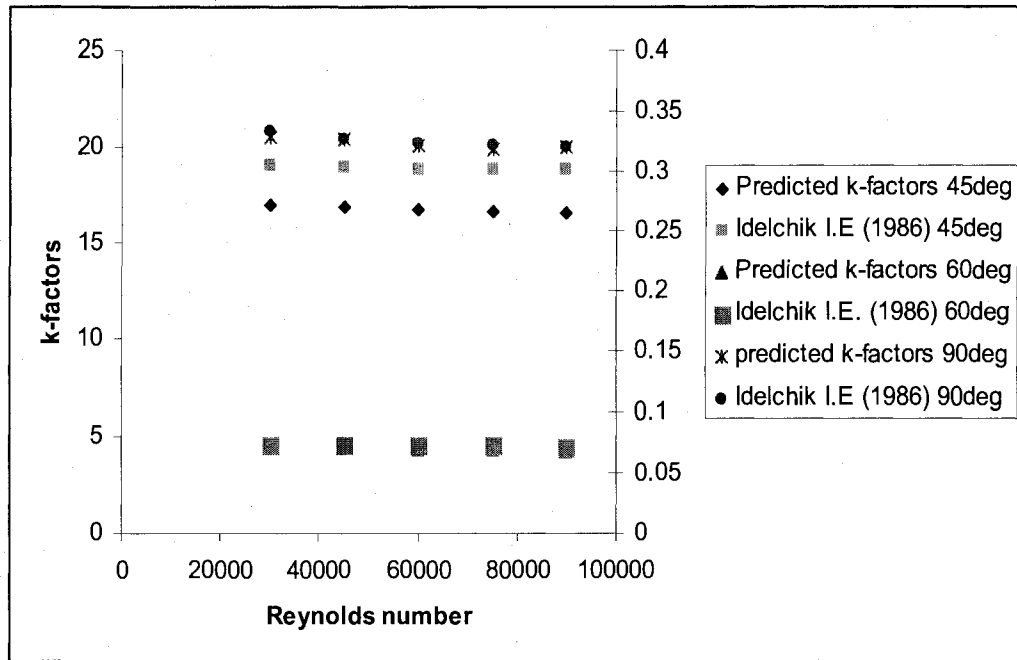


Figure 4 - 22 Comparison of k-factors at 45, 60 and 90 degree damper opening

Figure 4-23 compares the predicted values to the ones obtained from a research paper Gan G and Riffat S.B (1999). The authors studied a similar situation but for a square duct geometry. The values differ considerably owing to the difference in the geometry. From the graph it can be enumerated that the values of k-factors are lower for a circular duct at low angles of damper opening and become higher as the angle increases. When air flows over a flat plate damper (Gan G & Riffat S.B), the resulting sudden contraction and expansion is more predominant because of the sharp corners when compared to circular shaped dampers. This comparison shows that the pressure losses depend on the geometry of the duct and the damper. From the above plots, it is evident that the damper angle has more effect on the pressure loss coefficient than the Reynolds number. Though at higher Reynolds numbers, the magnitudes of velocity and pressure are high, the pressure loss coefficient does not vary much. This is due to the fact the increase in pressure drop

values are overlaid by the corresponding increase in the mean velocity of air flow with increased Reynolds numbers.

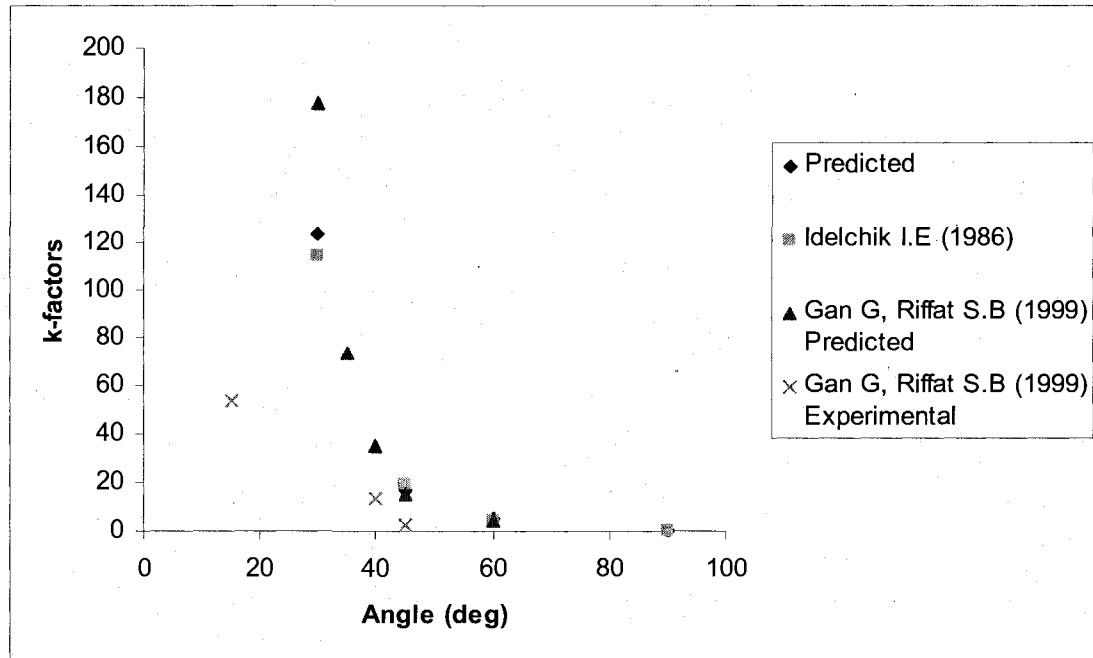


Figure 4 - 23 Comparison of k-factors at Re=90000

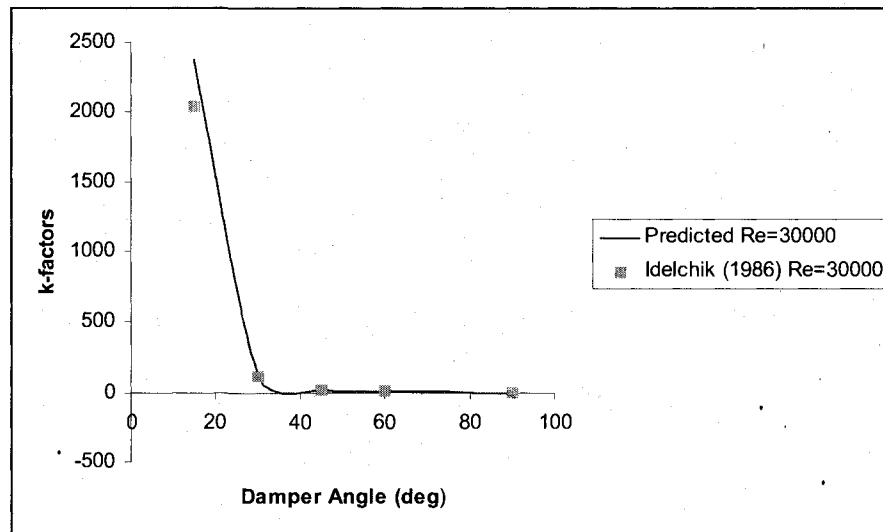


Figure 4 - 24 Comparison of k-factors at Re=30000

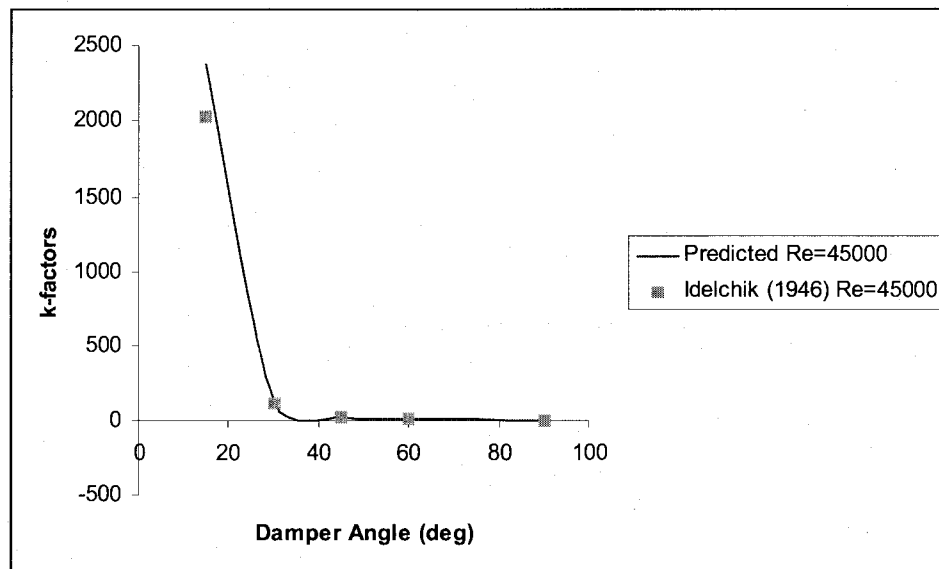


Figure 4 - 25 Comparison of k-factors at Re=45000

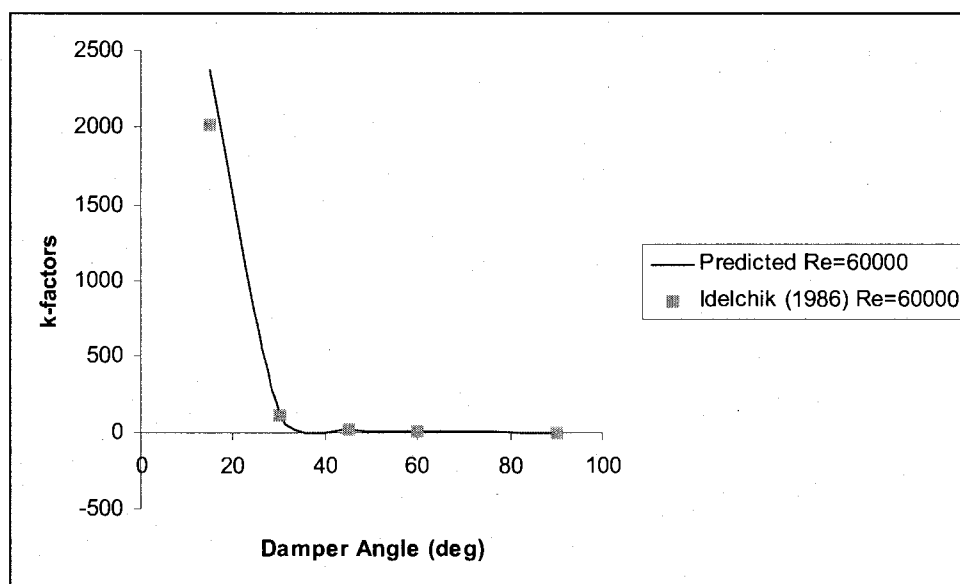


Figure 4 - 26 Comparison of k-factors at Re=60000

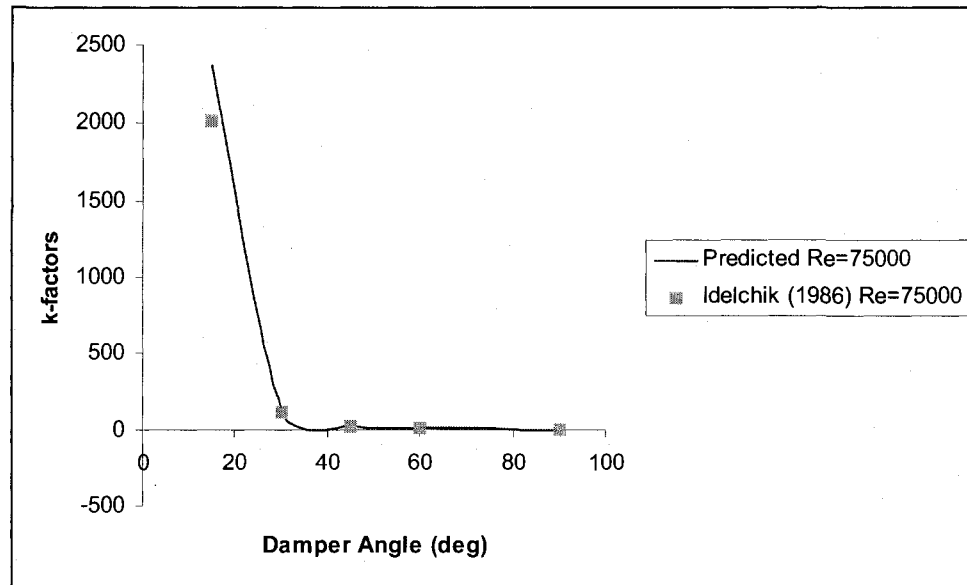


Figure 4 - 27 Comparison of k-factors at Re=75000

Figures 4-24, 4-25, 4-26, 4-27 compares the predicted k-factors and Idelchik (1986) at Re=30000, 45000, 60000 and 75000. It can be seen that the values at smaller angles differ slightly as explained previously. The Reynolds Number has little impact on the values of pressure loss coefficients in the considered Reynolds Numbers range.

From the study, it is clear that the pressure losses at small angles are very high. As the angle increases the pressure losses are reduced. The values of inlet velocities also slightly affect the flow. At high Reynolds numbers, flow separation occurs and recirculation zones are formed.

The main application of the results obtained from this research would be in the Direct Digital Control (DDC) systems. A pressure transducer can be taken as the input device to the DDC control loop. The pressure losses can be the input signal which would be processed by a predetermined program in the DDC loop and would then send signal to the damper actuator which in turn would change the position of the damper if necessary.

CHAPTER 5

CONCLUSIONS

Pressure loss coefficients for five different damper angles were studied over Reynolds numbers varying from 30000 to 90000 using the CFD simulation software Star-CD. A 3 dimensional model was developed, discretized and analyzed in Star-CD. The pressure loss coefficient which characterizes the pressure losses through the damper was determined by some post-processing. The obtained pressure loss coefficients were compared with Handbook values by Idelchik (1986) and also with a previous research work (Gan G., and Riffat S.B., 1999). The pressure loss coefficient was found to increase with increased damper opening. Reynolds number has a little impact on the k-factors. The k-factors slightly decreased with increasing Reynolds numbers. The predicted k-factor values were in general agreement with Idelchik (1986). The slight difference was due to the difference in the basic construction of the CFD model and the model employed by Idelchik.

The predicted k-factors values were compared with a research work done by Gan and Riffat who predicted the pressure loss coefficients for a square duct with a flat plate damper. The difference in the value suggested that the pressure losses are affected by the shape of the duct and the damper. Therefore to understand the pressure loss characteristics of dampers full knowledge of the shape and size of the duct and damper is essential. The agreement of the predicted results and Idelchik for a circular duct with

circular damper reiterates the importance of CFD tool in the prediction of pressure loss coefficients. As the types of dampers available are enormous, CFD can be accurately used as a tool for determining the pressure loss characteristics without the need of performing tedious experiments.

The study of the control part of the HVAC system can be an extension of the current research work. In addition, this study does not consider the clearance between the duct and the damper. In the future, the case where some clearance between the duct and the damper specified would be an interesting one to study and see the effect of clearance on the pressure loss coefficient.

REFERENCES

1. Shan K. Wang, Handbook of Air Conditioning and Refrigeration, McGraw-Gill, Inc., New York.
2. George Clifford, Modern Heating, Ventilating, and Air Conditioning, Prentice Hall, Englewood Cliffs, New Jersey.
3. Roger W. Haines, Lewis Wilson C., HVAC Systems Design Handbook, Third Edition, McGraw-Hill.
4. Jones W.P., Air Conditioning Engineering, Fourth Edition, Edward Arnold, London.
5. Gan G., and Riffat S.B., 1999. Determination of Energy Loss Characteristics of Dampers, International Journal of Energy Research, 23, 61-69.
6. Dickey P.S., and Cohan J.R., (1942). A study of Damper Characteristics, Trans. ASME, 64, 299.
7. Shao L., Riffat S.B., Accuracy of CFD for Predicting Losses in HVAC Duct Fittings, Applied Energy 51, 233-248, 1995.
8. Idelchik I. E., Handbook of Hydraulic Resistance, 1986, Hemisphere Publishing Corporation, Washington.
9. Damper automatic controls,
http://highperformancehvac.com/ddc_vav_systems.html, Accessed on August 1st, 2008

10. Faye C. Mcquiston, Jerald D. Parker, Jeffrey D. Spitler, Heating Ventilating and Air Conditioning Analysis and Design, Fifth Edition, John Wiley & Sons, Inc., New York.
11. Gan G., and Riffat S.B., CFD Prediction of k-factors of Duct Elbows, International Journal of Energy Research, Vol. 21, 675-681 (1997).
12. Koch P., Comparisons and choice of pressure loss coefficients, ζ for ductwork components, Building Serv. Eng. Res. Technol. 22,3 (2001) pp 167-183.
13. Launder B.E., and Spalding D.B., The Numerical Computation of Turbulent Flows, Computer methods in Applied Mechanics & Engineering 3, (1974) 269-289.
14. Legg, R.C. Characteristics of Single and Multi-blade Dampers for Ducted Air Systems, Building Services Engng. Res. Technol., 7 (4), 1986, 129-145.
15. Barron, R.M., and Ali A. Salehi Neyshabouri, Effects of Under-Relaxation Factors on Turbulent Flow Simulations, Int. Journal for Numerical Methods in Fluids, 2003, Vol 42, 923-928.
16. StarCD User Manual, Version 3.24 Adapco.
17. Gan G., and Riffat S.B., (1995) k-factors for HVAC Ducts-Numerical and Experimental Determination, BSER&T, 16(3), 133-139.
18. Saha S.K., and Mallic D.N., Heat Transfer and Pressure Drop Characteristics of Laminar Flow in Rectangular and Square Plain Ducts and Ducts with Twisted-Tape Inserts, Journal of Heat Transfer, 2005 Vol. 127, 966-977.

19. Cheong, K.W and Riffat S.B., A New Method for Determining of Velocity Pressure Loss-Factors for HVAC System Components. Proceedings 13th AIVC Conference, France, 1992, pp. 546-61.
20. Shih T H., Liou W.W., Shabbir A., and Zhun J., 1995, A New k- ϵ Eddy-Viscosity Model for High Reynolds Number Turbulent Flows – Model Development and Validation, Computer Fluids, Vol. 24, 227-238

VITA

Graduate College
University of Nevada, Las Vegas

Pallavi Annabattula

Local Address:

4235, Cottage Circle, Apt#4,
Las Vegas, Nevada, 89119

Degrees:

Bachelor of Engineering, Mechanical Engineering, 2006
Andhra University College of Engineering, India

Thesis Title:

A CFD model to predict pressure loss coefficient in circular ducts with a
motorized damper

Thesis Examination Committee:

Chairperson, Samir Moujaes, Ph.D, P.E.
Committee Member, Robert Boehm, Ph.D., P.E.,
Committee Member, Woosoon Yim, Ph.D.
Graduate Faculty Representative, Saman Ladkany, Ph.D., P.E.